Published in final edited form as:

Adv Parasitol. 2020 ; 107: 25–96. doi:10.1016/bs.apar.2019.11.001.

Microtubule organelles in *Giardia*

Kari D. Hagen, **Shane G. McInally**, **Nicholas D. Hilton**, **Scott C. Dawson***

Department of Microbiology and Molecular Genetics, UC Davis, Davis, CA, United States

Abstract

Giardia lamblia is a widespread parasitic protist with a complex MT cytoskeleton that is critical for motility, attachment, mitosis and cell division, and transitions between its two life cycle stages —the infectious cyst and flagellated trophozoite. *Giardia* trophozoites have both highly dynamic and highly stable MT organelles, including the ventral disc, eight flagella, the median body and the funis. The ventral disc, an elaborate MT organelle, is essential for the parasite's attachment to the intestinal villi to avoid peristalsis. *Giardia's* four flagellar pairs enable swimming motility and may also promote attachment. They are maintained at different equilibrium lengths and are distinguished by their long cytoplasmic regions and novel extra-axonemal structures. The functions of the median body and funis, MT organelles unique to *Giardia*, remain less understood. In addition to conserved MT-associated proteins, the genome is enriched in ankyrins, NEKs, and novel hypothetical proteins that also associate with the MT cytoskeleton. High-resolution ultrastructural imaging and a current inventory of more than 300 proteins associated with *Giardia's* MT cytoskeleton lay the groundwork for future mechanistic analyses of parasite attachment to the host, motility, cell division, and encystation/excystation. *Giardia's* unique MT organelles exemplify the capacity of MT polymers to generate intricate structures that are diverse in both form and function. Thus, beyond its relevance to pathogenesis, the study of *Giardia*'s MT cytoskeleton informs basic cytoskeletal biology and cellular evolution. With the availability of new molecular genetic tools to disrupt gene function, we anticipate a new era of cytoskeletal discovery in *Giardia*.

1. Introduction

Microbial eukaryotes often possess unique and elaborate microtubule (MT) organelles composed of both conserved MT binding proteins and novel proteins whose functions are unknown (Dawson and Paredez, 2013; Nosala et al., 2018). These novel proteins lack homology to known MT-associated proteins and may contribute to cytoskeletal architecture or to processes such as MT nucleation, assembly, or dynamics (Hagen et al., 2011; Hu et al., 2006; Preisner et al., 2016). Like other microbial eukaryotes, the diplomonad *Giardia lamblia* has a complex three-dimensional ultrastructure with several novel MT organelles and higher order structural elements of unknown function and composition (Fig. 1; Dawson, 2010). The primary cytoskeletal organelles in *Giardia* are the eight flagella and basal bodies, the ventral disc, the median body, and the funis and caudal complex (Fig. 1A–D; Dawson, 2010). *Giardia's* two nuclei undergo a semi-open mitosis in which the mitotic spindle forms

*Corresponding author: scdawson@ucdavis.edu.

around the nuclear envelope and kinetochore MTs segregate chromosomes (Sagolla et al., 2006). As compared to evolutionarily conserved and well-studied cytoskeletal structures such as the mitotic spindle or flagellum (Chaaban and Brouhard, 2017), *Giardia's* unique MT organelles illustrate the capacity of simple MT polymers to generate intricate structures that are diverse in both form and function.

Giardia's complex MT cytoskeleton is of critical importance throughout each of its life cycle stages—the cyst and the motile trophozoite (Nosala and Dawson, 2015). Cysts ingested by the mammalian host excyst in the small intestine. During excystation, beating of the flagella may aid in opening the cyst, allowing the slightly rounded, quadrinucleate excyzoite to emerge. The excyzoite then elongates and undergoes cytokinesis, producing two binucleate daughter cells (Buchel et al., 1987; Feely, 1986). The multiflagellated motile trophozoites attach to the intestinal microvilli using a unique MT organelle, the ventral disc (Dawson, 2010). Trophozoites colonise the small intestine, undergoing cell division approximately once every 6–8h. Prior to cytokinesis, new dual mitotic spindles segregate chromosomes and new MT structures (ventral disc, eight axonemes, etc.) are assembled and inherited. *Giardia* lacks an anaphase-promoting complex and many conserved mitotic checkpoint complex proteins (Vicente and Cande, 2014) found in other eukaryotes. In the absence of a canonical contractile ring, flagellar motility generates forces that drive daughter cells in opposing directions during cytokinesis (Hardin et al., 2017). As they transit through the intestinal tract, trophozoites eventually differentiate to become cysts (Roxstrom-Lindquist et al., 2006). Early in encystation, the two nuclei divide by a semi-open mitosis that occurs in the absence of cytokinesis, yielding a quadrinucleate precyst (Jirakova et al., 2012). Cytoskeletal movements, combined with the assembly of the cyst wall, remodel trophozoites from a flattened teardrop shape to the more ovoid shape characteristic of the cyst (Midlej and Benchimol, 2009). Each of the eight flagella are internalized during cyst formation, yet do not completely resorb (Midlej and Benchimol, 2009). The MT spiral of the ventral disc is fragmented and partially disassembled by unknown mechanisms. Mature cysts are then disseminated into the environment.

Giardia's MT cytoskeleton is thus essential for key aspects of its life cycle including motility, host attachment, intracellular transport, cell division, encystation, and excystation. It is also a critical determinant of cell shape, cell polarization, and intracellular trafficking. Beyond its clinical relevance, the study of *Giardia*'s MT cytoskeleton also informs basic cell biology, molecular biology and cellular evolution (Dawson, 2010). This chapter focuses on the structure, composition and dynamic movements of the primary MT cytoskeletal organelles in *Giardia*: the ventral disc, median body, and eight flagella and basal bodies.

2. Conserved and novel composition of the MT cytoskeleton

MTs are highly conserved cytoskeletal polymers composed of heterodimers of α- and β-tubulin. As polar polymers, MTs have two distinct ends—the plus and minus ends. Individual MT polymers exhibit intrinsic dynamic instability at the highly dynamic ends, where MTs exist either in growth (polymerization) or shrinkage (depolymerization) phases (Desai and Mitchison, 1997). The organization of MT arrays in cells is tightly controlled by MT-associated proteins (MAPs) that promote or suppress MT dynamic behaviour at the ends

to regulate overall rates of MT assembly and disassembly, as well as the frequencies of catastrophes and rescues (Akhmanova and Steinmetz, 2015). Centrosomes or basal bodies are the primary MT organizing centres (MTOCs) in cells, yet MTs may also nucleate by non-centrosomal methods. New MT filaments are formed by nucleation from the minus end, dependent on γ-tubulin ring complexes (γ-TuRCs) that comprise MTOCs (Moritz and Agard, 2001). MAPs such as the EB proteins (EB1), XMAP215, CLIP-170 and CLASP proteins regulate dynamics at the MT plus ends, and are termed MT plus-end tracking proteins (+TIPs). Microtubule motors such as kinesins and dyneins also regulate MT dynamics and organization by sliding and linking MTs along other existing filaments. Microtubule organization is also regulated through the MT-severing proteins katanin and spastin (McNally and Roll-Mecak, 2018). Lastly, numerous tubulin post-translational modifications (PTMs) influence polymer dynamics by tuning MAP activity and affinity (Song and Brady, 2015).

The *Giardia lamblia* (ATCC 50803) genome contains conserved structural cytoskeletal proteins (see Table 1), as well as proteins known to regulate MT nucleation (γ-TuRCs), stability, and dynamics (e.g. XMAP215, katanin, and EB1) or to post-translationally modify tubulin (e.g. tubulin tyrosine ligases). Many of these proteins associate with more than one cytoskeletal structure and certain protein families are highly represented (Fig. 1E and F). *Giardia* also has 24 kinesins and 14 dynein heavy chain motor proteins that may regulate MT dynamics or organelle trafficking in this complex cell. The genome also contains 21 annexin homologues (alpha-giardins) (Weiland et al., 2005), and nearly 200 NIMA (NEK) kinases (Manning et al., 2011), which are often associated with the cytoskeleton. Despite having an elaborate microtubule cytoskeleton, *Giardia* lacks the MARK (microtubule affinity-regulating kinase) and the microtubule-associated kinases MAST and TTBK (Tau tubulin kinase) (Manning et al., 2011). Together, conserved MAPs and motors, along with other *Giardia*-specific MAPs, regulate MT assembly, disassembly, dynamics and stability in each of the MT organelles (disc, flagella, median body, funis, and spindles).

During cell division, *Giardia's* two spindles are dynamic, and it is likely that the assembling disc, flagella, funis and median body are also subject to MT dynamics. While the flagella and median body are dynamic interphase arrays, the ventral disc is a highly stable structure that appears to lack canonical interphase MT dynamics. Whether the funis or caudal complex MTs are dynamic during interphase is unknown. Microtubule-disrupting and MT-stabilizing drugs are valuable tools to probe the assembly dynamics of MTs in *Giardia* by either sequestering tubulin monomer pools and inhibiting tubulin polymerization (nocodazole, colchicine, oryzalin) or by stabilizing growing MTs (Taxol) (Bhattacharyya et al., 2008; Pellegrini and Budman, 2005). Microtubules of the eight flagella, the median body, and the mitotic spindles are sensitive to these drugs, whereas the ventral disc MTs are unaffected (Sagolla et al., 2006) in interphase. Disc MTs are likely stabilized by MAPs that limit MT dynamics, as effects such as severe deformation of the disc are observed only after long incubation periods with MT destabilizing drugs that involve multiple rounds of cell division (Chavez et al., 1992; Oxberry et al., 1994). These findings are supported by the localization of known MAPs (EB1, XMAP215, and katanin) and motors (kinesins and dyneins) (Morrison et al., 2007) that regulate dynamics to the eight flagella, median body or spindles, but not to the ventral disc.

Molecular genetic strategies such as morpholino or CRISPRi knockdown and overexpression of dominant negative mutant proteins have been used to investigate the role of conserved MAPs and motors in *Giardia*. For example, knockdown or ectopic expression of a dominant negative kinesin-13 (a depolymerizing kinesin) results in flagellar length and median body defects (Dawson et al., 2007). Similar studies with kinesin-2a, part of the kinesin-2 heterotrimeric complex that delivers IFT particles to the flagellar tip, resulted in decreases in the lengths of the membrane-bound regions of the flagella, confirming its role in flagellar assembly and length maintenance in *Giardia* (Hoeng et al., 2008).

Giardia possesses a single homologue of the conserved MT plus-end tracking protein EB1, which regulates microtubule dynamics by recruiting other +TIPs to microtubule plus ends (Akhmanova and Steinmetz, 2015). In *Giardia*, EB1 is reported to localize to the nuclear envelope, the median body, the flagellar tips and the mitotic spindles of dividing trophozoites (Dawson et al., 2007; Kim et al., 2014). Morpholino knockdown of EB1 resulted in a reduction in the size of the median body, as well as an increase in the number of quadrinucleate trophozoites, suggesting a role in mitosis (Dawson et al., 2007; Kim et al., 2014). The interaction between EB1 and other +TIPs may depend on its phosphorylation state, and in vitro assays indicate a possible role for *Giardia* aurora kinase in EB1 phosphorylation (Kim et al., 2017). Yeast two-hybrid assays with EB1 identified additional interacting proteins, including γ-giardin (Kang et al., 2010), a component of the ventral disc microribbons. Morpholino knockdown of γ-giardin resulted in shortening of the microribbons and flattening of the ventral groove region of the disc (Kim and Park, 2019) confirming a structural role for γ-giardin; however, the role of EB1 in ventral disc MT dynamics remains unknown.

The role of γ-tubulin, a component of MT organizing centres (MTOCs), has also been examined in *Giardia* (Kim and Park, 2018). γ-tubulin is found in the MT nucleating γ-TuSC complex along with GCP2 and GCP3. γ-tubulin localizes primarily to *Giardia's* basal bodies, as well as to the flagella and mitotic spindles (Davids et al., 2011; Kim and Park, 2018; Nohynkova et al., 2000). Morpholino knockdown of γ-tubulin, GCP2 and GCP3 resulted in mitotic defects, decreases in both median body volume and caudal flagellar length, and an increase in abnormal axonemes lacking a central pair (Kim and Park, 2018). These effects were observed to a lesser extent for GCP2 and GCP3 knockdown, although the degree of protein depletion differed for each these knockdowns.

3. Complex architecture and composition of the ventral disc

The ventral disc is perhaps the defining organelle in *Giardia*—it is a prominent, suction-cup-shaped MT structure that facilitates parasite attachment (Fig. 2; Crossley and Holberton, 1983, 1985; Feely et al., 1982; Friend, 1966; Holberton, 1973a, 1981). Attachment to the host intestinal epithelium is essential for in vivo colonization. Using the ventral disc, trophozoites attach non-invasively to the microvilli, as well as to inert surfaces such as glass or plastic (reviewed recently in Nosala et al., 2018). *Giardia*'s attachment to surfaces is reversible and dynamic, allowing the parasite to resist peristaltic flow in the host gastrointestinal tract (Nosala et al., 2018).

The intricate architecture of the ventral disc and the complexity of the higher order structures associated with disc MTs were first described in the 1960s (Cheissin, 1964; Friend, 1966). In the past decade, however, cryo-electron tomography (cryo-ET) with subtomogram averaging yielded the first 3D high-resolution structure of the ventral disc and revealed dense protein complexes coating the protofilaments of the MT spiral array (Fig. 2A; Schwartz et al., 2012). The ventral disc comprises approximately 100 parallel, evenly spaced MTs that spiral clockwise around a central bare area and overlap to form a domed organelle 8 μm in diameter (Brown et al., 2016). Trilaminar structures called microribbons jut dorsally from the MT spiral, and vary in height and angle along the entire length of the array (Brown et al., 2016). The microribbons are thought to lend rigidity and stability to the domed disc structure (Holberton, 1973a, 1981; Schwartz et al., 2012), and are connected laterally at 16nm intervals by flexible structures known as crossbridges. Along the outer facing margin of disc are other MT-associated complexes (side-arms and paddles) that repeat every 8 nm and are thus spaced at the distance of a single alpha/beta-tubulin dimer (Schwartz et al., 2012). The disc MT array also includes other repetitive elements that may regulate organelle behaviour and confer stability (Ichikawa and Bui, 2018), such as the MT outer proteins (gMAPs 1–3) and inner proteins (gMIPs 5, 7 and 8) associated with the outer and inner MT walls (Schwartz et al., 2012). A small left-handed MT spiral array, the supernumerary MT array, lies dorsal to the main ventral disc structure and has no known function. Lastly, the lateral crest, associated with the disc margin, forms a seal with surfaces in early attachment (Feely et al., 1982, 1990; House et al., 2011) and may have contractile functions (Kulda and Nohynkova, 1995).

The identities and functions of the disc substructures and protein densities revealed by detailed cryo-ET must still be determined (Brown et al., 2016); however, progress in identifying numerous disc-associated proteins (DAPs) has been made using a combination of biochemical, proteomic and fluorescent-tagging approaches (reviewed in Nosala et al., 2018). Early biochemical studies with detergent extracted ventral discs showed that several ~30kDa DAPs, termed “giardins” to indicate their *Giardia* origin, copurified with tubulin and were likely components of the disc microribbons (Crossley and Holberton, 1983). More recently, we used a comprehensive proteomic approach with C-terminal GFP-tagging of disc protein candidates to identify nearly 20 new DAPs localizing to the disc and lateral crest (Hagen et al., 2011); through an ongoing project associated with the GiardiaDB (Aurrecoechea et al., 2009), the total number of DAPs localizing to the disc in interphase trophozoites now exceeds 90 (see Table 2; Nosala et al., 2018). Nearly two-thirds of known DAPs localize only to the disc, whereas the remainder also localize to other MT structures such as the flagellar axonemes, basal bodies, and median body (Fig. 1E). Regional variations in the disc ultrastructure that have been defined by cryo-ET (Brown et al., 2016) are mirrored in the localizations of DAPs to distinct areas of the disc, including the overlap zone, ventral groove, supernumerary MTs, MT nucleating dense bands and disc margin or lateral crest (Fig. 2A and B; Nosala et al., 2018).

The disc is primarily composed of ankyrins and novel hypothetical proteins that have no homology to proteins outside of *Giardia* species (Andersson et al., 2007; Fig. 1F). One such novel DAP, median body protein (MBP, DAP16343), is a major component of the disc spiral MT array and localizes strongly to the ventral disc edge and overlap zone. Both morpholino

and CRISPRi knockdowns result in open discs, demonstrating that MBP is necessary for proper ventral disc biogenesis and function (McInally et al., 2019; Woessner and Dawson, 2012). Nearly 30 DAPS are ankyrins, which contain 33-amino acid helix-turn-helix domains, often in tandem arrays, that act as molecular scaffolding to bring proteins together and mediate protein stability (Islam et al., 2018; Li et al., 2006). A few DAPs that may comprise the microribbons (Feely et al., 1990) are striated fibre (SF)–assemblins (beta-giardin, delta-giardin, and SALP-1) (Palm et al., 2003), whereas several others are “alpha-giardins” belonging to the annexin family of Ca2+ regulated membrane binding proteins that have diverse functions in cells (Bauer et al., 1999; Peattie, 1990; Weiland et al., 2003, 2005). At least 14 DAPs are NEKs (Table 2) kinases, which are associated with the cytoskeleton in other organisms (O’Regan et al., 2007). *Giardia lamblia* (ATCC 50803) has an expanded family of 198 NEKs, (Manning et al., 2011); however, nearly three-fourths of them lack conserved catalytic residues, making their role in the cell uncertain. In other eukaryotic cells, such pseudokinases may retain signalling functions as scaffolds or kinase substrates (Manning et al., 2011).

Despite the localization of some DAPs to multiple MT structures, only two DAPs have MT binding motifs or homology to known MAPs. One of the 24 *Giardia* kinesins—kinesin-6a (DAP102455)—localizes to disc margin, whereas DAP5374, a CAP-Gly protein, has a conserved MT binding motif (Weisbrich et al., 2007) and likely interacts with tubulin and MT lattices. DAP16263 is a homologue of DIP13, a MT-associated protein found in flagellates and other organisms with flagellated cell stages (Fritz-Laylin et al., 2010; Pfannenschmid et al., 2003). DAP16263 localizes to the flagella and ventral disc (Hagen et al., 2011), primarily to the overlap zone and ventral axonemes, but it lacks the conserved KREE binding domain that allows direct interaction with MTs (Pfannenschmid et al., 2003). In *Chlamydomonas*, DIP13 localizes to the centrioles and to cytoplasmic and flagellar MTs, and may stabilize or connect MTs to other cellular structures (Pfannenschmid et al., 2003).

The disc is “hyperstable” structure, as drugs that normally affect MT dynamic instability have no effect on ventral disc MTs (Dawson et al., 2007) and turnover of DAPs has not been observed (Hagen et al., 2011). The DAPs that coat both the outside and inside of nearly all disc MT protofilaments, including the gMAPs and gMIPs, likely confer hyperstability to the disc singlet MT array (Brown et al., 2016; Schwartz et al., 2012). DAPs may also nucleate the disc MT array, bind and stabilize MT plus and minus ends, or facilitate or stabilize the curvature and doming of the disc (Brown et al., 2016; Schwartz et al., 2012). Future molecular genetic and functional analyses of DAPs will be central towards understanding disc architecture, assembly and attachment dynamics.

4. Mechanisms of ventral disc-mediated attachment

Giardia attachment to surfaces is reversible and occurs within seconds. Using TIRF microscopy and *Giardia* trophozoites stained with a fluorescent membrane marker, the stages of attachment were defined based the degree of trophozoite contact with the attachment surface (House et al., 2011). During the earliest attachment stages, the trophozoite skims along the surface and makes mechanosensory contact using the ventrolateral flange. A seal then forms as the disc perimeter contacts the surface. In the later

stages of attachment, additional contacts are formed between the surface and the plasma membrane of the bare area and lateral shield regions. The lateral shield regions of the cell body lie alongside the ventral flagella, whereas the bare area region, which lacks MTs, is located in the centre of the disc array and contains numerous membrane-bound vacuoles (Friend, 1966).

Despite the critical role of parasite attachment by the ventral disc for *Giardia*'s pathogenesis (Nosala and Dawson, 2015), the evaluation of any proposed attachment mechanism has been limited by over 50 years of conflicting observations and theoretical biophysical models of attachment that lack corresponding empirical analyses (Feely and Erlandsen, 1981, 1982; Hansen et al., 2006; Hansen and Fletcher, 2008; Holberton, 1974; Inge et al., 1988; Mariante et al., 2005; Sousa et al., 2001). Various conformational changes in the disc may be required for either early or late stage suction-based attachment (House et al., 2011; Owen, 1980). The rigid structure of the ventral disc could also indirectly contribute to attachment by maintaining a negative pressure differential created by some other unknown mechanism (e.g., an osmotic pressure differential-based mechanism) (Friend, 1966; Hansen et al., 2006; Hansen and Fletcher, 2008). Proposed models of *Giardia* attachment to surfaces include: ligand-independent interactions (electrostatic or van der Waals forces) (Hansen et al., 2006), ligand-dependent interactions (Inge et al., 1988; Magne et al., 1991; Nash et al., 1983; Ortega-Barria et al., 1994; Sousa et al., 2001), clutching mechanisms (Feely and Erlandsen, 1981; Holberton, 1973a,b; Inge et al., 1988), or suction-mediated mechanisms (Feely and Erlandsen, 1981; Hansen et al., 2006; Hansen and Fletcher, 2008; Holberton, 1973a,b, 1974). Each of the proposed models is not necessarily mutually exclusive. Despite this diversity of attachment models, disc-mediated suction is likely sufficient for in vitro attachment (Hansen et al., 2006; Hansen and Fletcher, 2008).

For almost five decades, the "hydrodynamic suction model" of *Giardia* attachment has remained an unconfirmed, yet often cited mechanism of attachment by the ventral disc (Holberton, 1973a, 1974). As hypothesized by Holberton, the continuous beating of a trophozoite's ventral flagella lowers the pressure underneath a static, inflexible ventral disc, generating a hydrodynamic force sufficient for attachment. The hydrodynamic model was initially derived from observations of the murine isolate *G. muris* attached to glass slides, with subsequent mathematical modelling of fluid flow under low Reynolds number to confirm the theoretical feasibility of hydrodynamic suction (Holberton, 1974). The hydrodynamic model relies on a constantly open ventral groove region that is lacking in *Giardia muris* (Holberton, 1973b; Holberton and Ward, 1981). Holberton's hydrodynamic suction model of *Giardia* attachment is contingent on three essential requirements: (1) ventral flagellar beating establishes hydrodynamic flow underneath the disc through proposed channels at the disc perimeter; (2) continuous ventral flagellar beating is required to maintain a hydrodynamic suction through the open channels; and (3) the ventral disc must be concave, inflexible and rigid to accommodate the biophysical stresses of a negative pressure differential underneath the disc relative to the outside medium (Holberton, 1974).

For years, the key assumptions of the hydrodynamic model—such as the contribution of flagellar motility to hydrodynamic flow—were neither confirmed by direct live observations of human *Giardia* isolates nor evaluated using standard molecular genetic approaches. In

2011, however, House et al. showed that, once attached, *Giardia* mutants with severe defects in flagellar beating (ventral or any flagella) were able to resist shear and normal forces (House et al., 2011). While it remains possible that flagellar motility is required for early stages of attachment, proper ventral flagellar beating is not required for trophozoites to maintain their attachment to surfaces, which is incongruent with the second assumption of the hydrodynamic model. For hydrodynamic current to flow underneath the disc, the hydrodynamic model predicted the existence of open channels that direct current around the disc periphery (Holberton, 1974). In contrast to early descriptions of an unsealed disc, our lab's more recent quantitative time-lapse live TIRF imaging indicated the presence of a disc perimeter (or lateral crest) seal in *attached* trophozoites that are resistant to shear and normal forces (House et al., 2011). This lateral crest seal is not congruent with the proposed "lateral channels" (Holberton, 1974) that were deemed necessary to facilitate a hydrodynamic current around the disc perimeter in *G. muris* isolates (Woessner and Dawson, 2012). Disruptions of the lateral crest seal in a morpholino-based disc mutant also cause an open, flattened disc that limits the parasite's ability to resist shear or normal forces (Woessner and Dawson, 2012).

Seal formation during attachment is likely mediated by the lateral crest (House et al., 2011), a repetitive structure on the outer edge of the ventral disc that is composed of a network of fibres (Feely et al., 1982; Friend, 1966; Hagen et al., 2011). The presence of seal contacts demarks the transition from attaching trophozoites to attached trophozoites. Lateral crest DAPs, like other DAPs, are primarily proteins that are unique to *Giardia* or possess ankyrin repeat or NEK kinase domains (e.g. DAP13981). Actin was initially reported to localize to the lateral crest and periphery of the disc using heterologous (anti-chicken) antibodies (Feely et al., 1982), but this is likely an artefactual localization due to the divergence of the *Giardia* actin gene (Morrison et al., 2007). The subsequent use of *Giardia*-specific actin antibodies (Paredez et al., 2011) indicated that actin does not localize to the ventral disc or the lateral crest.

Given a wealth of new proteins associated with the ventral disc, future studies of disc-mediated attachment should include molecular genetic and biochemical analysis of DAPs, with the aim of resolving the long-standing controversies concerning the existence and the role of disc flexibility, curvature, and lateral crest seal formation in attaching trophozoites.

5. The structure and putative functions of the median body

The crooked *Giardia* "smile" is formed by the "median body", an MT array of unknown function (Dawson, 2010; Piva and Benchimol, 2004). The median body is a bundle of semi-organized MTs, located on the dorsal side of trophozoites, roughly perpendicular to the caudal axonemes and posterior to the ventral disc. Median body MTs are dynamic during interphase, as they are sensitive to both MT stabilizing and MT depolymerizing drugs (Dawson et al., 2007; Sagolla et al., 2006). Median body MT dynamics are also regulated by the depolymerizing kinesin motor protein kinesin-13 (Dawson et al., 2007). Thus is likely that the median body possesses a mixture of dynamic and more stable MTs.

Several clues to median body function derive from analyses of median body structure and shape throughout the life cycle. The shape and the presence of the median body varies during the cell cycle; it disappears altogether following mitosis, prior to disc division (Sagolla et al., 2006). The median body may serve as a reservoir of tubulin subunits for duplicating MT structures, such as the daughter ventral discs, prior to cytokinesis (Brugerolle, 1975; Feely et al., 1990). This would permit the rapid assembly of the ventral disc so that trophozoites could quickly reattach to the intestinal villi. In support of this hypothesis, Brugerolle identified small “appendages” similar to the disc microribbons on median body MTs (Brugerolle, 1975). In addition, Crossley et al. showed beta-giardin also localized to the median body of some cells (Crossley et al., 1986). Most recently, Hardin et al. (2017) observed the flux of mNeonGreen labelled tubulin from the median body to assembling microtubule structures including the spindles, daughter discs and nascent flagella in mitotic cells, supporting the “reservoir” hypothesis. An alternative function of the median body has also been proposed, implicating this structure in detachment (Piva and Benchimol, 2004). To date, the function of the median body remains enigmatic; few studies have investigated the “reservoir” hypothesis or this alternative “detachment” hypothesis.

6. Flagella and basal body architecture and composition

The discovery of *Giardia* is attributed to Antonie van Leewenhoek, (Dobell, 1932) who in 1681 observed teardrop shaped flagellates with “sundry little paws”. More than 300 years later, our understanding of *Giardia* flagellar biology remains rudimentary. Like all diplomonads, *Giardia* trophozoites have eight flagella that all retain the canonical “9+2” structure of the eukaryotic motile flagellum (Manton and Clarke, 1952). The eight flagella are organized into four symmetrical pairs: the anterior, the caudal, the posteriolateral, and the ventral (Fig. 1). The basal bodies that nucleate all flagella are located in the anterior of the cell between the two nuclei (Fig. 1; McInally and Dawson, 2016). The anterior basal bodies are located near the anterior ends of the two nuclei and are oriented towards the anterior end of the cell. Basal bodies that nucleate the ventral, caudal and posteriolateral axonemes are positioned posteriorly below the two anterior basal bodies and are oriented towards the posterior of the cell. The anterior axonemes cross over the ventral disc MT array before exiting on the right and left sides of the anterior ventrolateral flange. The length from the cell body to the flagellar tip is about 12μm. The two caudal axonemes run along the anterior-posterior axis of the cell, and measure about 7μm from the cell body to the distal tip. The ventral axonemes exit the cell body just posterior to the disc and extend about 14μm in the ventrocaudal groove, a channel bounded on either side by the lateral shield regions. Lastly, the posteriolateral axonemes angle outward at the lower third of the cell body, extending about 8μm from the cell body (Dawson and House, 2010).

In general, eukaryotic flagella extend from a basal body or centriole and are surrounded by a specialized flagellar membrane after they project from the cell surface. The conserved MT architecture of the axoneme consists of a central pair of singlet MTs surrounded by outer doublet MTs that are connected to one another by nexin links. The A tubules of the outer doublets have associated inner- and outer- dynein arms and radial spokes that project towards the central pair. In contrast to other flagellated protists, each *Giardia* axoneme has a long cytoplasmic region that extends from the centrally located basal body to the point

where it exits the cell body as a membrane-bound flagellum (Fig. 2C and D; see Dawson and House, 2010). These long cytoplasmic regions are not extended transition zones (Hoeng et al., 2008). In spite of the extensive cytoplasmic regions, *Giardia* axonemes have a conserved structure akin to more commonly studied flagella in experimental systems such as *Chlamydomonas*. Each of the eight *Giardia* axonemes retains the central pair and outer doublet MTs, dynein arms and radial spokes (Carvalho and Monteiro-Leal, 2004; Clark and Holberton, 1988). Electron-dense "flagellar pore complexes" are located at the regions where each flagellum exits the cell body, and likely form a diffusion barrier between the cytoplasmic and membrane-bound compartments of each axoneme (Hoeng et al., 2008). Inheritance of the eight axonemes is complex and is maintained through basal body migration, duplication, maturation, and subsequent association with the specific spindle poles during cell division (Nohynkova et al., 2006).

While flagellar and basal body proteomics has contributed to our overall understanding of flagellar structure and evolution in eukaryotes, these structures are difficult to isolate from the rest of the *Giardia* cytoskeleton (Lauwaet et al., 2011). Nonetheless, many flagellar proteins have been identified in the *Giardia* genome (Table 3) using proteomic and gene sequence analysis. It has been proposed that more than 500 proteins comprise the eukaryotic flagellum (Dutcher, 1995; Luck, 1984; Ostrowski et al., 2002; Pazour et al., 2005); however, some flagellar components appear to be lineage-specific. The *Giardia* genome contains over 100, MT-associated, flagellar and basal body proteins (see Table 3). Flagellar structural components include the protofilament ribbons (Rib43a and Rib72), the central pair (PF16, PF20, and hydin), the radial spokes (rsp3 and rsp9), and nexin links (PF2). Canonical basal body-associated proteins (e.g. centrin, delta-tubulin and epsilon-tubulin) and five components of the BBSome are also present (Table 3). Centrin localizes to two distinct clusters adjacent to the two nuclei during interphase, colocalizing with the flagellar basal bodies (Sagolla et al., 2006). Consistent with observations in other flagellated cells, γ-tubulin also localizes to flagellar basal bodies during interphase; however, γ-tubulin localization is restricted only to flagella that are newly produced during cell division (Nohynkova et al., 2006). Some proteins identified by comparative proteomics of basal body proteins lack basal body localization in *Giardia* (e.g. FAP52 GL50803_15956 and PACRG1 GL50803_15455), or localize to other MT structures as well as basal bodies (e.g. GL50803_8557 and GL50803_29796) (McInally and Dawson, 2016). *Giardia* also has basal body-localizing proteins that lack homology to known basal body proteins in other eukaryotes (e.g. GL50803_15193 and GL50803_6254) (McInally and Dawson, 2016). In total, over 70 proteins have been shown to localize to some or all *Giardia* basal bodies (see McInally and Dawson, 2016; Fig. 1; Table 3).

More than 1000 hypothetical proteins (e.g., those lacking significant similarity to proteins in other organisms) have been identified in the *Giardia* genome. This genetic novelty is reflected in the analyses of basal body (Lauwaet et al., 2011) and flagellar proteomes (Hagen et al., 2011) and by the fact that the majority of proteins known to localize to the axonemes and basal bodies are hypothetical (Fig. 1F). Each basal body and axoneme is unique in its cytological position and its association with different cytoskeletal structures, including extra-axonemal structures. To date, several pairs of axonemes have specific proteins that localize exclusively to either the cytoplasmic or membrane-bound regions.

Such proteins include GASP-180, a member of a novel family of coiled-coil proteins (Elmendorf et al., 2003), and several members of the multi-gene α-giardin family (Kim et al., 2013; Szkodowska et al., 2002; Wei et al., 2010; Weiland et al., 2005; Wu et al., 2016). The α-giardins are related to annexins—calcium-dependent phospholipid-binding proteins that may serve to anchor other proteins to the plasma membrane (Rescher and Gerke, 2004). Whether these *Giardia* annexins contribute to flagellar function or structure is unknown (Vahrmann et al., 2008).

7. Putative functions of axoneme-associated structures

Novel axoneme-associated structures (Friend, 1966) define each flagellar pair. Specifically, the cytoplasmic portions of the anterior axonemes are associated with dense rods, and are connected to the “marginal plates” by a system of filaments (Friend, 1966; Maia-Brigagao et al., 2013); electron dense material is associated with cytoplasmic regions of the posteriolateral axonemes; “caudal complex” or “funis” microtubules surround and extend from the caudal axonemes; and fin-like structures extend from membrane-bound regions of the ventral axonemes (Kulda and Nohynkova, 1995). Although our understanding of the composition and function of these axoneme-associated structures is limited, each confers a unique structural identity to the different flagellar pairs and, likely, enables functional differentiation with respect to motility or even attachment (Campanati et al., 2002). For example, the “marginal plate” and “striated fibre” structures associated with the cytoplasmic regions of the anterior axonemes are located slightly dorsal to the anterior regions of the disc spiral array (Kulda and Nohynkova, 1995). These structures are in close proximity to the ventral disc, and may affect or modulate disc conformational dynamics and attachment. Likewise, the composition or dynamics of the funis and caudal complex, which are associated with the cytoplasmic regions of the caudal axonemes, are unclear. Funis and caudal complex MTs form sheets that are likely nucleated from bands of linked MTs in the nuclear region of the caudal basal bodies (Benchimol et al., 2004). The funis MTs wrap the caudal axonemes near the basal bodies, then fan out laterally at the emergence of the ventral axonemes (Benchimol et al., 2004). Microtubule plus ends of the funis may to be anchored in the cytoplasmic regions of the posteriolateral axonemes, and filamentous links of funis MTs to the underlying plasma membrane are also reported (Benchimol et al., 2004). The funis and caudal complex may limit the movements of caudal flagella (Campanati et al., 2002), and have been suggested to either have a structural role in maintaining cell shape or a potential role in generating movements of the posterior “tail” region during detachment (Benchimol et al., 2004; Carvalho and Monteiro-Leal, 2004; Ghosh et al., 2001; Owen, 1980). Lastly, the fin-like structures associated with the ventral flagella give these flagella a unique shape that may contribute to attachment by evacuating fluid from beneath ventral disc and by providing a downward force that drives the ventral disc towards the surface (Lenaghan et al., 2011).

8. Flagellar motility and role during the life cycle

The coordinated beating of *Giardia’s* eight motile flagella results in complex movements essential for motility and cell division, and may aid in parasite attachment to the host gut epithelium (Fig. 3; Campanati et al., 2002; Dawson and House, 2010). Modelling and

analysis of the flagellar movements of unattached trophozoites (Lenaghan et al., 2011, 2013) showed that rapidly swimming cells exhibit rotational or tumbling movements accompanied by undulations of the caudal region that may propel the cell forward. Tumbling motion ceases and movement becomes stable and planar during the transition to attachment (Lenaghan et al., 2011). During planar movement, the ventral flagella provide propulsive force for turning and forward motion, and the anterior flagella provide steering and control (Lenaghan et al., 2013). Not all flagellar pairs have characteristic flagellar waveforms (Campanati et al., 2002). The ventral flagella beat in an expanding sinusoidal waveform due to the boundary conditions imposed by the ventral groove, whereas the anterior and posteriolateral flagellar pairs beat in a paddle-like fashion with a strong downward power stroke followed by a reduced drag upstroke (Lenaghan et al., 2011). Despite having a motile "9+2" axonemal structure, the cytoplasmic regions of caudal axonemes flex rather than beat with a canonical flagellar waveform, and external regions of the caudal axonemes are non-motile. This absence of beating has been attributed to the presence of the caudal complex surrounding the cytoplasmic regions of the caudal axonemes. The "tail" region of trophozoites bends dorsally as well as laterally, a motion termed "dorsolateral tail flexion" (Carvalho and Monteiro-Leal, 2004). This tail flexion derives from the sliding of MTs of the caudal complex, caudal axonemes, or funis (Campanati et al., 2002). Ventral flagellar beating, as mentioned above, has also been implicated in the generation of suction-based attachment via the "hydrodynamic model" (Holberton, 1974).

Flagellar beating has thus been argued to be essential for the maintenance of attachment, and conversely the cessation of flagellar beating has been proposed as the mechanism of parasite detachment (Cheissin, 1964; Holberton, 1973a,b, 1974). Whether these observations reflect causality (ventral flagellar beating causes attachment) or correlation (ventral flagella beat at the same time cells attach) is unknown. Thus the role of ventral flagellar beating in attachment remains open to debate. Early attachment models invoked ventral flagellar beating as a means to generate a hydrodynamic force (Holberton, 1974) to create suction. Recent studies modelling *Giardia* motility suggest that the ventral flagella are ideally suited both for providing a downward force that drives the disc towards the attachment surface and for removing fluid from underneath the ventral disc (Lenaghan et al., 2011, 2013). Even if it is not required to generate hydrodynamic currents, flagellar motility is essential for positioning the cell parallel to surfaces prior to attachment and for manoeuvring trophozoites towards suitable niches for colonization. Future mechanistic studies should consider the relative contributions of both disc conformational dynamics and flagellar motility to attachment.

9. Flagellar assembly and equilibrium length maintenance

Eukaryotic flagella are dynamic, membrane-bound and compartmentalized MT-based organelles that facilitate diverse cellular behaviours including motility and chemosensation (Brooks and Wallingford, 2014; Pazour and Witman, 2003). Early work in the green alga *Chlamydomonas reinhardtii* showed that axonemes are assembled by the addition of proteins at the distal flagellar tip, rather than at the basal body (Kozminski et al., 1993). Axonemal building blocks are trafficked to the tip using a bidirectional process called intraflagellar transport (IFT) (Kozminski et al., 1993; Lechtreck, 2015), in which proteinaceous particles

or “trains” synthesized in the cytoplasm are continuously carried to and from the tip by MT motor proteins (Rosenbaum and Witman, 2002; Scholey, 2003). Both flagellar assembly and length maintenance are dependent upon the active transport of protein complexes by IFT (Kozminski et al., 1993; Marshall et al., 2005). IFT components—including IFT particles, the BBsome, kinesin and dynein motors, and transition zone (TZ) complex proteins—are widely conserved in free-living and parasitic unicellular flagellates (Buisson et al., 2013; Hao et al., 2009; Kozminski et al., 1993).

Like many model organisms, *Giardia* has canonical motile axonemes that are nucleated by basal bodies and have a conserved “9+2” axoneme structure. Yet in contrast to other models, the eight *Giardia* axonemes are paired into four flagellar types with four different equilibrium lengths and include long, non-membrane-bound cytoplasmic regions (Fig. 4A and B). *Giardia* also possesses the majority of IFT, BBSome, and motor proteins (kinesin-2, kinesin-13, and IFT dynein) that are essential components of flagellar length control mechanisms in diverse model systems (Avidor-Reiss and Leroux, 2015; Lechtreck, 2015). *Giardia* axonemes lack a transition zone, however, and there are no TZ protein homologues in the genome (Avidor-Reiss and Leroux, 2015; Barker et al., 2014).

The anterograde movement of IFT trains along the outer doublet of axonemes to the flagellar tip is mediated by the kinesin-2 heterotrimeric complex, which is comprised of two kinesin-2 homologues and the kinesin-associated protein (KAP). The retrograde movement of IFT rafts back towards the cell body is mediated by cytoplasmic dynein 1b (Orozco et al., 1999). Proteins homologous to components of the retrograde and anterograde IFT complexes (A and B), the kinesin-II heterotrimeric complex and IFT dynein are found in *Giardia* (see Table 3). The primary anterograde IFT motor in *Giardia* is the kinesin-2 heterotrimeric complex (Briggs et al., 2004; Morrison et al., 2007. In *Giardia*, both IFT complex A and B components localize to the cytoplasmic and membrane-bound regions of axonemes (Fig. 4C and D). Kinesin-2 GFP fusions (*GiKIN2a* and *GiKIN2b*) and components of the IFT complex A (IFT140) and complex B (IFT81) raft localize along the length of cytoplasmic axonemes and form foci at the eight distal flagellar tips and the flagellar pore complex regions (Hoeng et al., 2008).

Cytoplasmic regions of axonemes, including the non-motile caudal pair, have a conserved flagellar ultrastructure, possessing the outer doublet MTs, canonical radial spokes, axonemal dynein arms and the central MT pair (Carvalho and Monteiro-Leal, 2004; Clark and Holberton, 1988). Cytoplasmic axoneme length is unaffected by morpholinos that interfere with kinesin-2 expression or by the overexpression of a dominant negative kinesin-2 (Carpenter and Cande, 2009; Hoeng et al., 2008). This is also supported by CRISPRi-mediated knockdown of kinesin-2 (McInally et al., 2019). IFT trains likely diffuse on cytoplasmic portions of axonemes, and accumulate and inject into the membrane-bound portions at the flagellar pore complexes (Hoeng et al., 2008). IFT-mediated axoneme assembly appears to be required only for membrane-bound regions of axonemes. Overall, these studies imply that cytoplasmic axonemes are assembled by an IFT-independent mechanism. Both IFT-mediated and non-IFT mediated assembly of axonemes can occur simultaneously in the same cell (Briggs et al., 2004). The mechanism and temporal sequence

by which the extra-axonemal-associated structures (e.g. marginal plate, fins, caudal complex or funis) are assembled during cell division remains unclear (Hoeng et al., 2008).

The lengths of flagella are dynamic, and steady-state or equilibrium flagellar length is a balance between IFT-mediated flagellar assembly and flagellar disassembly. A classic experiment in the green alga *Chlamydomonas* known as the "long-zero" experiment showed that amputation of one of the two flagella led to equalization of the lengths of both flagella due to a shared, limited precursor pool for regrowth. This and subsequent studies in *Chlamydomonas* have been used to develop the "balance-point model" of flagellar length regulation (Marshall and Rosenbaum, 2001). According to this model, constitutively controlled steady-state length is a balance between a *length-dependent assembly* rate and a *length-independent disassembly* rate. Equilibrium length is altered through modulating the rates of flagellar assembly or disassembly.

While flagellar assembly and length regulation is well-studied in some model systems, little is known about how flagella with different equilibrium lengths are assembled and regulated in the same cell. In *Giardia*, hierarchical levels of regulation must act to maintain four different flagellar lengths. We have recently shown that IFT-mediated flagellar assembly is length-independent, as IFT train size, speed, and injection frequencies are similar between flagella of different lengths (McInally et al., 2020). Axonemal MT disassembly is mediated by action of kinesin-13, a depolymerizing kinesin. Overexpression of a dominant negative kinesin-13 or CRISPRi-mediated kinesin-13 knockdown results in long flagella (Dawson et al., 2007; McInally et al., 2019). Equilibrium flagellar length is also sensitive to both MT stabilizing and destabilizing drugs (Dawson et al., 2007). Treatment with the MT stabilizing drug Taxol resulted in all flagella extending over three times the average interphase length (Dawson et al., 2007). Overall in *Giardia*, kinesin-13 mediates a disassembly-driven, length-dependent mechanism of length regulation that balances length-independent IFT-mediated assembly, resulting in different lengths (McInally et al., 2020).

10. Assembly and inheritance of MT organelles during cell division

Mitosis occurs in 6.5min and new daughter discs and new flagella are assembled in less than 3 min (Hardin et al., 2017). The two spindles radiate from one of the flagellar basal bodies near each spindle pole, forming a sheath around the nuclear envelope. Each spindle pole is associated with at least one axoneme. The nuclear envelope remains, forming a barrier between cytoplasmic MT arrays and chromatin; there is no evidence of mixing of the chromatin between nuclei (Sagolla et al., 2006). Daughter cells inherit one copy of each parent nucleus. Presumptive kinetochore MTs penetrate at the spindle poles through large polar openings in the nuclear membrane (Sagolla et al., 2006). Likely more than one MT is attached per kinetochore in *Giardia*. The internal (presumably kinetochore) MTs extend only a few microns into the nucleus near the chromatin in late stage (anaphase B) nuclei.

During mitosis, trophozoites remain attached from the onset of cell division through the assembly of the new daughter discs (Nohynkova et al., 2000; Tumova et al., 2007). In late mitosis, the parental disc undergoes dramatic structural changes, leading to parental ventral disc disassembly and detachment prior to the late stages of cytokinesis. Before parental disc

disassembly occurs, the two daughter discs are assembled de novo on the anterior dorsal side of the attached parent cell, with their ventral sides exposed on the parental cell surface (Tumova et al., 2007). Assembly of daughter discs is thought to terminate after the detachment of the dividing cell (Tumova et al., 2007). The amount of polymerized tubulin is nearly tripled in dividing cells (Brown et al., 2016).

Before mitosis is completed, flagellar and basal body duplication occurs (Nohynkova et al., 2006; Sagolla et al., 2006). Flagellar regeneration begins in anaphase with short flagella (presumably the new ventral and posteriolateral pairs) emerging from the spindle poles (Nohynkova et al., 2006; Sagolla et al., 2006). *Giardia*'s eight basal bodies have a unique inheritance pattern in daughter cells. In the interphase trophozoite, eight basal bodies are arranged into two tetrads and each basal body pair is associated with a distinct flagellum. The polarity of each daughter cell is thought to be determined through the association of axonemal basal bodies with the dividing nuclei (Sagolla et al., 2006).

Due to the inheritance and de novo assembly of specific flagella in daughter cells, a multigenerational division cycle has been proposed in *Giardia* wherein the relative age of a flagellar axoneme is different based on the anatomical position in the trophozoite (Nohynkova et al., 2006). The flagella of some other protists are known to undergo a similar maturation process that takes more than one cell cycle (Beech et al., 1991), mirroring the behaviour of centrioles in metazoans (reviewed in Beisson and Wright, 2003). Based on immunostaining with a polyglycylated tubulin antibody to visualize parental axonemes and an acetylated tubulin antibody to visualize daughter axonemes, eight parental (old) flagella are retained and eight new flagella are synthesized each cell division cycle (Nohynkova et al., 2006). While specific molecular markers have not been used to track each flagellar pair to confirm their identity during division (Nohynkova et al., 2006), the full length parental anterior axonemes are proposed to become the right caudal axonemes in the new daughter cells. Parental right caudal axonemes are then proposed to become the left caudal axonemes. Thus each daughter cell inherits a full complement of eight axonemes and associated basal bodies—four parental (old), and four newly duplicated each generation (Nohynkova et al., 2006; Sagolla et al., 2006). The timing and mechanism by which the extra-axonemal-associated structures (e.g. marginal plate, caudal complex or funis) are assembled during cell division also remains unclear (Hoeng et al., 2008).

The division of the caudal axonemes and their associated basal bodies also has notable implications for the de novo nucleation and assembly of the daughter ventral discs. After the daughter nuclei are partitioned and the caudal flagellar basal bodies have been repositioned between the two nuclei (Nohynkova et al., 2006), two new dorsal daughter ventral discs are assembled during telophase. The parental ventral disc is not disassembled until later in the cell cycle. Thus the caudal basal bodies nucleate the caudal axonemes and also determine the site of ventral disc assembly, establishing the polarity of the new daughter cells. The left caudal flagellum has been proposed to nucleate the spiral MT arrays that form the basis of the ventral disc (Friend, 1966); however, recent work shows that the dense bands near the basal bodies nucleate the ventral disc MTs (Brown et al., 2016; see Fig. 2).

Following mitosis, the ventral disc appears to be rapidly nucleated in at least four ways. Recent cryo-ET studies indicated that about 59% of ventral disc MTs are nucleated near the eight basal bodies (Brown et al., 2016). Disc MT minus ends do not directly contact basal bodies but rather arise from a series of perpendicular bands termed the dense band (DB) nucleation zone (Brown et al., 2016). The protein composition of these dense bands and the mechanism by which they support MT nucleation is undefined, although we have identified several proteins localizing to this region (Fig. 1). *Giardia* lacks some components of the gamma-TuRC nucleation complex yet retains the two gamma-TuSC components and gamma-tubulin (McInally and Dawson, 2016). Despite lacking an augmin homologue, about 39% of disc MTs nevertheless nucleate from the disc margin (DM) region, possibly via a branching nucleation-type mechanism (Brown et al., 2016). A small subset of MTs (~2%) is nucleated within the disc MT array itself. Lastly, an additional subset of about 20MTs nucleate from a distinct yet overlapping array of dense bands dorsal to the ventral disc, termed the supernumerary MTs (SN). This array is hypothesized to nucleate a new ventral disc during cell division, but this hypothesis fails to fully explain ventral disc biogenesis because two new discs are generated instead of one (Tumova et al., 2007).

The mechanism underlying the synchronized bending of newly growing disc MTs and the control of their length is also unknown. During dorsal daughter disc assembly, the MT spiral is nucleated first, with subsequent assembly and lengthening of the disc microribbons. The lateral crest is the last of the disc substructures to be assembled (Tumova et al., 2007). Assembling daughter discs appear to have varying levels of competence for attachment. As daughter discs assemble, the parental disc opens, and the spiral MT array disassembles. This process is accompanied by the progressive shortening and loss of the microribbons and the degradation of crossbridges. The final release of the disc from the basal bodies coincides with parental disc disassembly, and results in parasite detachment (Hardin et al., 2017; Tumova et al., 2007).

Dividing trophozoites not only need to build new daughter discs, but must also assemble other MT-based structures including two spindles and eight new flagella. Thus, the ventral disc MTs must be distinguished from the MTs of other MT arrays to properly recruit proteins required for the assembly of disc substructures. One obvious way that ventral disc MTs could be marked is by tubulin post-translational modifications (PTMs) (Garnham and Roll-Mecak, 2012), which could mediate the recruitment of DAPs to the nucleating disc during cell division. Disc substructures assemble sequentially on two daughter disc MT arrays in mitosis and excystation, yet the molecular details of this process are unclear (Palm et al., 2005; Tumova et al., 2007). Several regulatory proteins localize to the disc during division, including the sole *Giardia* aurora kinase (Davids et al., 2008), two putatively cell cycle-specific NEK kinases (Davids et al., 2011), and an ERK1 kinase that localizes to the disc during encystation (Ellis et al., 2003). Understanding how the ventral disc is assembled and which substructures and associated DAPs are essential for functional competency is critical for selecting potential druggable disc targets that may disrupt attachment and parasite colonization.

11. Assembly and inheritance of organelles during encystation and excystation

With respect to both encystation and excystation, the molecular genetic mechanisms underlying cytoskeletal assembly, disassembly, and cytoskeletal movements remain virtually undescribed. Encystation and excystation require flagellar, disc, and median body disassembly and assembly; however, the details or stages of cytoskeletal assembly/disassembly dynamics during these important transitions in the life cycle have not been described at the cytological or molecular level.

In the host, rounded excyzoites excyst from the cyst stage, then progressively elongate, and complete cytokinesis to differentiate into the motile trophozoites that colonise the small intestine (Buchel et al., 1987; Feely, 1986). The subsequent assembly of fully functional flagella and ventral discs allows the trophozoite to swim and attach to surfaces. As compared to encystation, the cytoskeletal changes that occur during the stages of excystation are less well characterized; however, cytoskeletal dynamics obviously play an important role in excystation. Flagellar motility has been suggested to play a mechanical role in the initial opening of the cyst. Other contractile or MT-mediated forces may also occur during excystation (Buchel et al., 1987; Feely, 1986). Prior to excystation, the trophozoite may undergo meiosis and nuclear fusion (Poxleitner et al., 2008).

Cytoskeletal movements, in conjunction with the assembly of the cyst wall, transform trophozoites into the environmentally resistant cyst form. Trophozoites transform from their characteristic teardrop shape to an ovoid shape as the cyst wall is assembled and cytoskeletal rearrangements occur during encystation (Midlej and Benchimol, 2009). The ventral disc structure transforms from a closed spiral disc to a horseshoe-shaped structure, then is subsequently fragmented and partially disassembled. Flagella are internalized and may continue to beat inside the newly formed cyst (Midlej and Benchimol, 2009).

12. Perspectives for future studies of *Giardia*'s MT organelles

Cytoskeletal innovation and diversity are widespread in eukaryotic cells (Dawson and Paredez, 2013), and *Giardia* and other diverse emerging cell biological model systems offer a wealth of unexplored MT structures with unique functional properties (Russell et al., 2017). Given the finite and relatively small number of known proteins that regulate MT dynamics and assembly, how do diverse eukaryotic cells like *Giardia* create elaborate MT structures?

The complex architecture and functions of the ventral disc and axoneme-associated structures challenge our conceptions of the capabilities of cytoskeletal polymers. As most efforts to study the *Giardia* cytoskeleton have been cytological, future work should emphasize understanding details of *Giardia*'s elaborate MT-based structures and elucidating the molecular mechanisms of dynamic cytoskeletal movements. The mechanisms of some *Giardia*-specific MT dynamics—such as attachment, cell division, and encystation/excystation—are essentially uncharacterized at the molecular level. Our identification and subcellular localization of several hundred proteins associated with disc, axonemes, basal

bodies, and median body lays the foundation for further analyses of MT assembly and function in *Giardia*. In vitro biochemical studies of novel MT-associated proteins in *Giardia* will aid in understanding their roles in modulating MT dynamics and regulation in the various MTs organelles.

The lack of forward genetic tools for *Giardia* has limited our ability to define genes that are required for cytoskeletal biology. Molecular genetic tools in *Giardia* include transient translational repression by electroporation of morpholinos (Carpenter and Cande, 2009) or the overexpression of long double-stranded RNAs or hammerhead ribozymes for transcriptional repression (Chen et al., 2007; Dan et al., 2000). While CRISPR/Cas9-mediated knockout strategies have recently been used for genome engineering in several parasitic protists (Ren and Gupta, 2017), our lab's recent development of CRISPRi-mediated transcriptional repression will advance studies of the *Giardia* cytoskeleton (McInally et al., 2019). Our successful use of CRISPRi to repress both exogenous, and single or multiple endogenous genes underscores the versatility of this stable and modular gene regulation methodology. CRISPRi knockdowns with partial transcriptional repression facilitate the identification of cytoskeletal genes with severe fitness costs (e.g. cell division or motility), as the complete knockdown or knockout of essential genes results in lethal phenotypes. We anticipate that the use of untargeted, genome-wide CRISPRi screens (Kampmann, 2018; Larson et al., 2013) could identify essential genes critical for *Giardia* growth and division, attachment, motility, and pathogenesis.

Acknowledgements

This work was supported by an NIH/NIAID award R01AI077571 to S.C.D. S.G.M. was supported by NIH T32 GM0007377. We also thank the numerous undergraduate researchers in our laboratory over the past 6 years who have contributed to creating and imaging GFP-tagged strains for GiardiaDB.

References

Akhmanova A, Steinmetz MO, 2015. Control of microtubule organization and dynamics: two ends in the limelight. Nat. Rev. Mol. Cell Biol 16 (12), 711–726. [PubMed: 26562752]

Andersson JO, Sjogren AM, Horner DS, Murphy CA, Dyal PL, Svard SG, Logsdon JM Jr., Ragan MA, Hirt RP, Roger AJ, 2007. A genomic survey of the fish parasite *Spironucleus salmonicida* indicates genomic plasticity among diplomonads and significant lateral gene transfer in eukaryote genome evolution. BMC Genomics 8, 51. [PubMed: 17298675]

Aurrecoechea C, Brestelli J, Brunk BP, Carlton JM, Dommer J, Fischer S, Gajria B, Gao X, Gingle A, Grant G, Harb OS, Heiges M, Innamorato F, Iodice J, Kissinger JC, Kraemer E, Li W, Miller JA, Morrison HG, Nayak V, Pennington C, Pinney DF, Roos DS, Ross C, Stoeckert CJ Jr., Sullivan S, Treatman C, Wang H, 2009. GiardiaDB and TrichDB: integrated genomic resources for the eukaryotic protist pathogens Giardia lamblia and *Trichomonas vaginalis*. Nucleic Acids Res. 37 (Database issue), D526–D530. [PubMed: 18824479]

Avidor-Reiss T, Leroux MR, 2015. Shared and distinct mechanisms of compartmentalized and cytosolic ciliogenesis. Curr. Biol 25 (23), R1143–R1150. [PubMed: 26654377]

Baker DA, Holberton DV, Marshall J, 1988. Sequence of a giardin subunit cDNA from Giardia lamblia. Nucleic Acids Res. 16 (14B), 7177. [PubMed: 3405761]

Barker AR, Renzaglia KS, Fry K, Dawe HR, 2014. Bioinformatic analysis of ciliary transition zone proteins reveals insights into the evolution of ciliopathy networks. BMC Genomics 15, 531. [PubMed: 24969356]

Bauer B, Engelbrecht S, Bakker-Grunwald T, Scholze H, 1999. Functional identification of alpha 1-giardin as an annexin of *Giardia lamblia*. FEMS Microbiol. Lett 173 (1), 147–153. [PubMed: 10220891]

Beech PL, Heimann K, Melkonian M, 1991. Development of the flagellar apparatus during the cell cycle in unicellular algae. Protoplasma 164 (1–3), 23–37.

Beisson J, Wright M, 2003. Basal body/centriole assembly and continuity. Curr. Opin. Cell Biol 15 (1), 96–104. [PubMed: 12517710]

Belhadri A, 1995. Presence of centrin in the human parasite Giardia: a further indication of its ubiquity in eukaryotes. Biochem. Biophys. Res. Commun 214 (2), 597–601. [PubMed: 7677770]

Benchimol M, Piva B, Campanati L, de Souza W, 2004. Visualization of the funis of *Giardia lamblia* by high-resolution field emission scanning electron microscopy—new insights. J. Struct. Biol 147 (2), 102–115. [PubMed: 15193639]

Bhattacharyya B, Panda D, Gupta S, Banerjee M, 2008. Anti-mitotic activity of colchicine and the structural basis for its interaction with tubulin. Med. Res. Rev 28 (1), 155–183. [PubMed: 17464966]

Briggs LJ, Davidge JA, Wickstead B, Ginger ML, Gull K, 2004. More than one way to build a flagellum: comparative genomics of parasitic protozoa. Curr. Biol 14 (15), R611–R612. [PubMed: 15296774]

Brooks ER, Wallingford JB, 2014. Multiciliated cells. Curr. Biol 24 (19), R973–R982. [PubMed: 25291643]

Brown JR, Schwartz CL, Heumann JM, Dawson SC, Hoenger A, 2016. A detailed look at the cytoskeletal architecture of the *Giardia lamblia* ventral disc. J. Struct. Biol 194 (1), 38–48. [PubMed: 26821343]

Brugerolle G, 1975. Contribution à l' étude cytologique et phylétique des diplozoaires (Zoomastigophorea, Diplozoa, Dangeard 1910). V. Nouvelle interpretation de l'organisation cellulaire de Giardie. Protistologica 11, 99–109.

Buchel LA, Gorenflot A, Chochillon C, Savel J, Gobert JG, 1987. In vitro excystation of Giardia from humans: a scanning electron microscopy study. J. Parasitol 73 (3), 487–493. [PubMed: 3598798]

Buisson J, Chenouard N, Lagache T, Blisnick T, Olivo-Marin JC, Bastin P, 2013. Intraflagellar transport proteins cycle between the flagellum and its base. J. Cell Sci 126 (Pt. 1), 327–338. [PubMed: 22992454]

Campanati L, Holloschi A, Troster H, Spring H, de Souza W, Monteiro-Leal LH, 2002. Video-microscopy observations of fast dynamic processes in the protozoon *Giardia lamblia*. Cell Motil. Cytoskeleton 51 (4), 213–224. [PubMed: 11977095]

Campanati L, Troester H, Monteiro-Leal LH, Spring H, Trendelenburg MF, de Souza W, 2003. Tubulin diversity in trophozoites of Giardia lamblia. Histochem. Cell Biol 119 (4), 323–331. [PubMed: 12687378]

Carpenter ML, Cande WZ, 2009. Using morpholinos for gene knockdown in *Giardia intestinalis*. Eukaryot. Cell 8 (6), 916–919. [PubMed: 19377039]

Carvalho KP, Monteiro-Leal LH, 2004. The caudal complex of Giardia lamblia and its relation to motility. Exp. Parasitol 108 (3–4), 154–162. [PubMed: 15582512]

Chaaban S, Brouhard GJ, 2017. A microtubule bestiary: structural diversity in tubulin polymers. Mol. Biol. Cell 28 (22), 2924–2931. [PubMed: 29084910]

Chavez B, Cedillo-Rivera R, Martinez-Palomo A, 1992. *Giardia lamblia*: ultrastructural study of the in vitro effect of benzimidazoles. J. Protozool 39 (4), 510–515. [PubMed: 1403986]

Cheissin EM, 1964. Ultrastructure of *Lamblia duodenalis*. I. Body surface, sucking disc and median bodies. J. Protozool 11, 91–98. [PubMed: 14119567]

Chen L, Li J, Zhang X, Liu Q, Yin J, Yao L, Zhao Y, Cao L, 2007. Inhibition of krr1 gene expression in *Giardia canis* by a virus-mediated hammerhead ribozyme. Vet. Parasitol 143 (1), 14–20. [PubMed: 16982153]

Clark JT, Holberton DV, 1988. Triton-labile antigens in flagella isolated from *Giardia lamblia*. Parasitol. Res 74 (5), 415–423. [PubMed: 3413040]

Crossley R, Holberton DV, 1983. Characterization of proteins from the cytoskeleton of *Giardia lamblia*. J. Cell Sci 59, 81–103. [PubMed: 6863412]

Crossley R, Holberton DV, 1985. Assembly of 2.5 nm filaments from giardin, a protein associated with cytoskeletal microtubules in *Giardia*. J. Cell Sci 78, 205–231. [PubMed: 4093472]

Crossley R, Marshall J, Clark JT, Holberton DV, 1986. Immunocytochemical differentiation of microtubules in the cytoskeleton of *Giardia lamblia* using monoclonal antibodies to alpha-tubulin and polyclonal antibodies to associated low molecular weight proteins. J. Cell Sci 80, 233–252. [PubMed: 3522613]

Dan M, Wang AL, Wang CC, 2000. Inhibition of pyruvate-ferredoxin oxidoreductase gene expression in *Giardia lamblia* by a virus-mediated hammerhead ribozyme. Mol. Microbiol 36 (2), 447–456. [PubMed: 10792730]

Davids BJ, Williams S, Lauwaet T, Palanca T, Gillin FD, 2008. *Giardia lamblia* aurora kinase: a regulator of mitosis in a binucleate parasite. Int. J. Parasitol 38 (3–4), 353–369. [PubMed: 17964578]

Davids BJ, Gilbert MA, Liu Q, Reiner DS, Smith AJ, Lauwaet T, Lee C, McArthur AG, Gillin FD, 2011. An atypical proprotein convertase in *Giardia lamblia* differentiation. Mol. Biochem. Parasitol 175 (2), 169–180. [PubMed: 21075147]

Dawson SC, 2010. An insider's guide to the microtubule cytoskeleton of *Giardia*. Cell. Microbiol 12 (5), 588–598. [PubMed: 20184590]

Dawson SC, House SA, 2010. Life with eight flagella: flagellar assembly and division in *Giardia*. Curr. Opin. Microbiol 13 (4), 480–490. [PubMed: 20580308]

Dawson SC, Paredez AR, 2013. Alternative cytoskeletal landscapes: cytoskeletal novelty and evolution in basal excavate protists. Curr. Opin. Cell Biol 25 (1), 134–141. [PubMed: 23312067]

Dawson SC, Sagolla MS, Mancuso JJ, Woessner DJ, House SA, Fritz-Laylin L, Cande WZ, 2007. Kinesin-13 regulates flagellar, interphase, and mitotic microtubule dynamics in *Giardia intestinalis*. Eukaryot. Cell 6 (12), 2354–2364. [PubMed: 17766466]

Desai A, Mitchison TJ, 1997. Microtubule polymerization dynamics. Annu. Rev. Cell Dev. Biol 13, 83–117. [PubMed: 9442869]

Dobell C, 1932. Antony van Leeuwenhoek and His "Little animals" Being Some Account of the Father of Protozoology and Bacteriology and His Multifarious Discoveries in These Disciplines; Collected, Translated, and Edited, From His Printed Works, Unpublished Manuscripts, and Contemporary Records. J. Bale sons & Danielsson ltd., London.

Dutcher SK, 1995. Flagellar assembly in two hundred and fifty easy-to-follow steps. Trends Genet. 11 (10), 398–404. [PubMed: 7482766]

Ebneter JA, Hehl AB, 2014. The single epsin homolog in Giardia lamblia localizes to the ventral disk of trophozoites and is not associated with clathrin membrane coats. Mol. Biochem. Parasitol 197 (1–2), 24–27. [PubMed: 25286382]

Ellis JG, Davila M, Chakrabarti R, 2003. Potential involvement of extracellular signal-regulated kinase 1 and 2 in encystation of a primitive eukaryote, *Giardia lamblia*. Stage-specific activation and intracellular localization. J. Biol. Chem 278 (3), 1936–1945. [PubMed: 12397063]

Elmendorf HG, Dawson SC, McCaffery JM, 2003. The cytoskeleton of *Giardia lamblia*. Int. J. Parasitol 33 (1), 3–28. [PubMed: 12547343]

Elmendorf HG, Rohrer SC, Khoury RS, Bouttenot RE, Nash TE, 2005. Examination of a novel head-stalk protein family in *Giardia lamblia* characterised by the pairing of ankyrin repeats and coiled-coil domains. Int. J. Parasitol 35 (9), 1001–1011. [PubMed: 15982656]

Feely DE, 1986. A simplified method for in vitro excystation of *Giardia muris*. J. Parasitol 72 (3), 474–475. [PubMed: 3746569]

Feely DE, Erlandsen SL, 1981. Isolation and purification of *Giardia* trophozoites from rat intestine. J. Parasitol 67 (1), 59–64. [PubMed: 7229820]

Feely DE, Erlandsen SL, 1982. Effect of cytochalasin-B, low Ca ++ concentration, iodoacetic acid, and quinacrine-HCl on the attachment of *Giardia* trophozoites *in vitro*. J. Parasitol 68 (5), 869–873. [PubMed: 7131192]

Feely DE, Schollmeyer JV, Erlandsen SL, 1982. *Giardia* spp.: distribution of contractile proteins in the attachment organelle. Exp. Parasitol 53 (1), 145–154. [PubMed: 7056342]

Feely DE, Holberton DV, Erlandsen SL, 1990. The biology of *Giardia*. In: Meyer EA (Ed.), Giardiasis. Human Parasitic Diseases. Elsevier, Amsterdam, pp. 11–50.

Friend DS, 1966. The fine structure of *Giardia muris*. J. Cell Biol 29 (2), 317–332. [PubMed: 5961344]

Fritz-Laylin LK, Prochnik SE, Ginger ML, Dacks JB, Carpenter ML, Field MC, Kuo A, Paredez A, Chapman J, Pham J, Shu S, Neupane R, Cipriano M, Mancuso J, Tu H, Salamov A, Lindquist E, Shapiro H, Lucas S, Grigoriev IV, Cande WZ, Fulton C, Rokhsar DS, Dawson SC, 2010. The genome of *Naegleriagruberi* illuminates early eukaryotic versatility. Cell 140 (5), 631–642. [PubMed: 20211133]

Garnham CP, Roll-Mecak A, 2012. The chemical complexity of cellular microtubules: tubulin post-translational modification enzymes and their roles in tuning microtubule functions. Cytoskeleton (Hoboken) 69 (7), 442–463. [PubMed: 22422711]

Ghosh S, Frisardi M, Rogers R, Samuelson J, 2001. How Giardia swim and divide. Infect. Immun 69 (12), 7866–7872. [PubMed: 11705969]

Hagen KD, Hirakawa MP, House SA, Schwartz CL, Pham JK, Cipriano MJ, De La Torre MJ, Sek AC, Du G, Forsythe BM, Dawson SC, 2011. Novel structural components of the ventral disc and lateral crest in *Giardia intestinalis*. PLoS Negl. Trop. Dis 5 (12), e1442. [PubMed: 22206034]

Hansen WR, Fletcher DA, 2008. Tonic shock induces detachment of *Giardia lamblia*. PLoS Negl. Trop. Dis 2 (2), e169. [PubMed: 18270543]

Hansen WR, Tulyathan O, Dawson SC, Cande WZ, Fletcher DA, 2006. *Giardia lamblia* attachment force is insensitive to surface treatments. Eukaryot. Cell 5 (4), 781–783. [PubMed: 16607025]

Hao L, Acar S, Evans J, Ou G, Scholey JM, 2009. Analysis of intraflagellar transport in C. elegans sensory cilia. Methods Cell Biol 93, 235–266. [PubMed: 20409821]

Harb OS, Roos DS, 2015. The eukaryotic pathogen databases: a functional genomic resource integrating data from human and veterinary parasites. Methods Mol. Biol 1201, 1–18. [PubMed: 25388105]

Hardin WR, Li R, Xu J, Shelton AM, Alas GCM, Minin VN, Paredez AR, 2017. Myosin-independent cytokinesis in Giardia utilizes flagella to coordinate force generation and direct membrane trafficking. Proc. Natl. Acad. Sci. U. S. A 114 (29), E5854–E5863. [PubMed: 28679631]

Hoeng JC, Dawson SC, House SA, Sagolla MS, Pham JK, Mancuso JJ, Lowe J, Cande WZ, 2008. High-resolution crystal structure and in vivo function of a kinesin-2 homologue in *Giardia intestinalis*. Mol. Biol. Cell 19 (7), 3124–3137. [PubMed: 18463165]

Holberton DV, 1973a. Fine structure of the ventral disk apparatus and the mechanism of attachment in the flagellate *Giardia muris*.J. Cell Sci 13 (1), 11–41. [PubMed: 4729933]

Holberton DV, 1973b. Mechanism of attachment of *Giardia* to the wall of the small intestine. Trans. R. Soc. Trop. Med. Hyg 67 (1), 29–30.

Holberton DV, 1974. Attachment of *Giardia*-a hydrodynamic model based on flagellar activity. J. Exp. Biol 60 (1), 207–221. [PubMed: 4594683]

Holberton DV, 1981. Arrangement of subunits in microribbons from *Giardia*. J. Cell Sci 47, 167–185. [PubMed: 7263776]

Holberton DV, Ward AP, 1981. Isolation of the cytoskeleton from *Giardia*. Tubulin and a low-molecular-weight protein associated with microribbon structures. J. Cell Sci 47, 139–166. [PubMed: 7263775]

House SA, Richter DJ, Pham JK, Dawson SC, 2011. Giardia flagellar motility is not directly required to maintain attachment to surfaces. PLoS Pathog. 7 (8), e1002167. [PubMed: 21829364]

Hu K, Johnson J, Florens L, Fraunholz M, Suravajjala S, DiLullo C, Yates J, Roos DS, Murray JM, 2006. Cytoskeletal components of an invasion machine—the apical complex of *Toxoplasma gondii*. PLoS Pathog. 2 (2), e13. [PubMed: 16518471]

Ichikawa M, Bui KH, 2018. Microtubule inner proteins: a meshwork of luminal proteins stabilizing the doublet microtubule. Bioessays 40 (3), 1700209.

Inge PM, Edson CM, Farthing MJ, 1988. Attachment of *Giardia lamblia* to rat intestinal epithelial cells. Gut 29 (6), 795–801. [PubMed: 3384364]

Islam Z, Nagampalli RSK, Fatima MT, Ashraf GM, 2018. New paradigm in ankyrin repeats: beyond protein-protein interaction module. Int. J. Biol. Macromol 109, 1164–1173. [PubMed: 29157912]

Jirakova K, Kulda J, Nohynkova E, 2012. How nuclei of Giardia pass through cell differentiation: semi-open mitosis followed by nuclear interconnection. Protist 163 (3), 465–479. [PubMed: 22209008]

Kampmann M, 2018. CRISPRi and CRISPRa screens in mammalian cells for precision biology and medicine. ACS Chem. Biol 13 (2), 406–416. [PubMed: 29035510]

Kang K, Kim J, Yong TS, Park SJ, 2010. Identification of end-binding 1 (EB1) interacting proteins in *Giardia lamblia*. Parasitol. Res 106 (3), 723–728. [PubMed: 19953272]

Keller LC, Romijn EP, Zamora I, Yates JR 3rd, Marshall WF, 2005. Proteomic analysis of isolated chlamydomonas centrioles reveals orthologs of ciliary-disease genes. Curr. Biol 15 (12), 1090–1098. [PubMed: 15964273]

Kim J, Park SJ, 2018. Roles of end-binding 1 protein and gamma-tubulin small complex in cytokinesis and flagella formation of *Giardia lamblia*. Microbiologyopen 8, e748.

Kim J, Park SJ, 2019. Role of gamma-giardin in ventral disc formation of *Giardia lamblia*. Parasit. Vectors 12 (1), 227. [PubMed: 31088539]

Kim J, Lee HY, Lee MA, Yong TS, Lee KH, Park SJ, 2013. Identification of alpha-11 giardin as a flagellar and surface component of *Giardia lamblia*. Exp. Parasitol 135 (2), 227–233. [PubMed: 23891940]

Kim J, Nagami S, Lee KH, Park SJ, 2014. Characterization of microtubule-binding and dimerization activity of *Giardia lamblia* end-binding 1 protein. PLoS One 9 (5), e97850. [PubMed: 24828878]

Kim J, Lee HY, Lee KH, Park SJ, 2017. Phosphorylation of serine 148 in *Giardia lamblia* end-binding 1 protein is important for cell division. J. Eukaryot. Microbiol 64 (4), 464–480. [PubMed: 27859890]

Kozminski KG, Johnson KA, Forscher P, Rosenbaum JL, 1993. A motility in the eukaryotic flagellum unrelated to flagellar beating. Proc. Natl. Acad. Sci. U. S. A 90 (12), 5519–5523. [PubMed: 8516294]

Kulda J, Nohynkova E, 1995. Giardia in humans and animals. In: Kreier JP (Ed.), Parasitic Protozoa. Academic Press, Inc., San Diego, pp. 225–423.

Larson MH, Gilbert LA, Wang X, Lim WA, Weissman JS, Qi LS, 2013. CRISPR interference (CRISPRi) for sequence-specific control of gene expression. Nat. Protoc 8 (11), 2180–2196. [PubMed: 24136345]

Lauwaet T, Davids BJ, Torres-Escobar A, Birkeland SR, Cipriano MJ, Preheim SP, Palm D, Svard SG, McArthur AG, Gillin FD, 2007. Protein phosphatase 2A plays a crucial role in *Giardia lamblia* differentiation. Mol. Biochem. Parasitol 152 (1), 80–89. [PubMed: 17204341]

Lauwaet T, Smith AJ, Reiner DS, Romijn EP, Wong CC, Davids BJ, Shah SA, Yates JR 3rd, Gillin FD, 2011. Mining the *Giardia* genome and proteome for conserved and unique basal body proteins. Int. J. Parasitol 41 (10), 1079–1092. [PubMed: 21723868]

Lechtreck KF, 2015. IFT-cargo interactions and protein transport in cilia. Trends Biochem. Sci 40 (12), 765–778. [PubMed: 26498262]

Lenaghan SC, Davis CA, Henson WR, Zhang Z, Zhang M, 2011. High-speed microscopic imaging of flagella motility and swimming in *Giardia lamblia* trophozoites. Proc. Natl. Acad. Sci. U. S. A 108 (34), E550–E558. [PubMed: 21808023]

Lenaghan SC, Chen J, Zhang M, 2013. Modeling and analysis of propulsion in the multiflagellated micoorganism *Giardia lamblia*. Phys. Rev. E Stat. Nonlinear Soft Matter Phys 88 (1), 012726.

Li J, Mahajan A, Tsai MD, 2006. Ankyrin repeat: a unique motif mediating protein-protein interactions. Biochemistry 45 (51), 15168–15178. [PubMed: 17176038]

Luck DJ, 1984. Genetic and biochemical dissection of the eucaryotic flagellum. J. Cell Biol 98 (3), 789–794. [PubMed: 6230366]

Magne D, Favennec L, Chochillon C, Gorenflot A, Meillet D, Kapel N, Raichvarg D, Savel J, Gobert JG, 1991. Role of cytoskeleton and surface lectins in *Giardia duodenalis* attachment to Caco2 cells. Parasitol. Res 77 (8), 659–662. [PubMed: 1805208]

Maia-Brigagao C, Gadelha AP, de Souza W, 2013. New associated structures of the anterior flagella of *Giardia duodenalis*. Microsc. Microanal 19 (5), 1374–1376. [PubMed: 24001879]

Manning G, Reiner DS, Lauwaet T, Dacre M, Smith A, Zhai Y, Svard S, Gillin FD, 2011. The minimal kinome of *Giardia lamblia* illuminates early kinase evolution and unique parasite biology. Genome Biol. 12 (7), R66. [PubMed: 21787419]

Manton I, Clarke B, 1952. An electron microscope study of the spermatozoid of sphagnum. J. Exp. Bot 3, 265–275.

Mariante RM, Vancini RG, Melo AL, Benchimol M, 2005. *Giardia lamblia*: evaluation of the *in vitro* effects of nocodazole and colchicine on trophozoites. Exp. Parasitol 110 (1), 62–72. [PubMed: 15804380]

Marshall WF, Rosenbaum JL, 2001. Intraflagellar transport balances continuous turnover of outer doublet microtubules: implications for flagellar length control. J. Cell Biol 155 (3), 405–414. [PubMed: 11684707]

Marshall WF, Qin H, Rodrigo Brenni M., Rosenbaum JL, 2005. Flagellar length control system: testing a simple model based on intraflagellar transport and turnover. Mol. Biol. Cell 16 (1), 270–278. [PubMed: 15496456]

McInally SG, Dawson SC, 2016. Eight unique basal bodies in the multi-flagellated diplomonad *Giardia lamblia*. Cilia 5, 21. [PubMed: 27379179]

McInally SG, Hagen KD, Nosala C, Williams J, Nguyen K, Booker J, Jones K, Dawson SC, 2019. Robust and stable transcriptional repression in *Giardia* using CRISPRi. Mol. Biol. Cell 30 (1), 119–130. [PubMed: 30379614]

McInally SG, Kondev J, Dawson SC, 2020. Length-dependent disassembly maintains four different flagellar lengths in Giardia. eLife(8) in press.

McNally FJ, Roll-Mecak A, 2018. Microtubule-severing enzymes: from cellular functions to molecular mechanism. J. Cell Biol 217 (12), 4057–4069. [PubMed: 30373906]

Meng TC, Aley SB, Svard SG, Smith MW, Huang B, Kim J, Gillin FD, 1996. Immunolocalization and sequence of caltractin/centrin from the early branching eukaryote Giardia lamblia. Mol. Biochem. Parasitol 79 (1), 103–108. [PubMed: 8844677]

Merchant SS, Prochnik SE, Vallon O, Harris EH, Karpowicz SJ, Witman GB, Terry A, Salamov A, Fritz-Laylin LK, Marechal-Drouard L, Marshall WF, Qu LH, Nelson DR, Sanderfoot AA, Spalding MH, Kapitonov VV, Ren Q, Ferris P, Lindquist E, Shapiro H, Lucas SM, Grimwood J, Schmutz J, Cardol P, Cerutti H, Chanfreau G, Chen CL, Cognat V, Croft MT, Dent R, Dutcher S, Fernandez E, Fukuzawa H, Gonzalez-Ballester D, Gonzalez-Halphen D, Hallmann A, Hanikenne M, Hippler M, Inwood W, Jabbari K, Kalanon M, Kuras R, Lefebvre PA, Lemaire SD, Lobanov AV, Lohr M, Manuell A, Meier I, Mets L, Mittag M, Mittelmeier T, Moroney JV, Moseley J, Napoli C, Nedelcu AM, Niyogi K, Novoselov SV, Paulsen IT, Pazour G, Purton S, Ral JP, Riano-Pachon DM, Riekhof W, Rymarquis L, Schroda M, Stern D, Umen J, Willows R, Wilson N, Zimmer SL, Allmer J, Balk J, Bisova K, Chen CJ, Elias M, Gendler K, Hauser C, Lamb MR, Ledford H, Long JC, Minagawa J, Page MD, Pan J, Pootakham W, Roje S, Rose A, Stahlberg E, Terauchi AM, Yang P, Ball S, Bowler C, Dieckmann CL, Gladyshev VN, Green P, Jorgensen R, Mayfield S, Mueller-Roeber B, Rajamani S, Sayre RT, Brokstein P, et al., 2007. The Chlamydomonas genome reveals the evolution of key animal and plant functions. Science 318 (5848), 245–250. [PubMed: 17932292]

Midlej V, Benchimol M, 2009. Giardia lamblia behavior during encystment: how morphological changes in shape occur. Parasitol. Int 58 (1), 72–80. [PubMed: 19073279]

Moritz M, Agard DA, 2001. Gamma-tubulin complexes and microtubule nucleation. Curr. Opin. Struct. Biol 11 (2), 174–181. [PubMed: 11297925]

Morrison HG, McArthur AG, Gillin FD, Aley SB, Adam RD, Olsen GJ, Best AA, Cande WZ, Chen F, Cipriano MJ, Davids BJ, Dawson SC, Elmendorf HG, Hehl AB, Holder ME, Huse SM, Kim UU, Lasek-Nesselquist E, Manning G, Nigam A, Nixon JE, Palm D, Passamaneck NE, Prabhu A, Reich CI, Reiner DS, Samuelson J, Svard SG, Sogin ML, 2007. Genomic minimalism in the early diverging intestinal parasite *Giardia lamblia*. Science 317 (5846), 1921–1926. [PubMed: 17901334]

Nash TE, Gillin FD, Smith PD, 1983. Excretory-secretory products of *Giardia lamblia*. J. Immunol 131 (4), 2004–2010. [PubMed: 6619547]

Nohria A, Alonso RA, Peattie DA, 1992. Identification and characterization of gamma giardin and the gamma giardin gene from *Giardia lamblia*. Mol. Biochem. Parasitol 56 (1), 27–37. [PubMed: 1474999]

Nohynkova E, Draber P, Reischig J, Kulda J, 2000. Localization of gamma-tubulin in interphase and mitotic cells of a unicellular eukaryote, *Giardia intestinalis*. Eur. J. Cell Biol 79 (6), 438–445. [PubMed: 10928459]

Nohynkova E, Tumova P, Kulda J, 2006. Cell division of *Giardia intestinalis*: flagellar developmental cycle involves transformation and exchange of flagella between mastigonts of a diplomonad cell. Eukaryot. Cell 5 (4), 753–761. [PubMed: 16607022]

Nosala C, Dawson SC, 2015. The critical role of the cytoskeleton in the pathogenesis of Giardia. Curr. Clin. Microbiol. Rep 2 (4), 155–162. [PubMed: 27347476]

Nosala C, Hagen KD, Dawson SC, 2018. 'Disc-o-Fever': getting down with Giardia's groovy microtubule organelle. Trends Cell Biol. 28 (2), 99–112. [PubMed: 29153830]

Nosala C, Hagen KD, Hilton N, Jones K, Loudermilk R, Nguyen K, Dawson SC, 2019. Disc-associated proteins (DAPs) mediate the unusual hyperstability of Giardias ventral disc. BioRxiv 361105.

O'Regan L, Blot J, Fry AM, 2007. Mitotic regulation by NIMA-related kinases. Cell Div. 2, 25. [PubMed: 17727698]

Orozco JT, Wedaman KP, Signor D, Brown H, Rose L, Scholey JM, 1999. Movement of motor and cargo along cilia. Nature 398 (6729), 674. [PubMed: 10227290]

Ortega-Barria E, Ward HD, Keusch GT, Pereira MEA, 1994. Growth inhibition of the intestinal parasite *Giardia lamblia* by a dietary lectin is associated with arrest of the cell cycle. J. Clin. Investig 94 (6), 2283–2288. [PubMed: 7989583]

Ostrowski LE, Blackburn K, Radde KM, Moyer MB, Schlatzer DM, Moseley A, Boucher RC, 2002. A proteomic analysis of human cilia: identification of novel components. Mol. Cell. Proteomics 1 (6), 451–465. [PubMed: 12169685]

Owen RL, 1980. The ultrastructural basis of Giardia function. Trans. R. Soc. Trop. Med. Hyg 74 (4), 429–433. [PubMed: 7445035]

Oxberry ME, Thompson RC, Reynoldson JA, 1994. Evaluation of the effects of albendazole and metronidazole on the ultrastructure of *Giardia duodenalis, Trichomonas vaginalis* and *Spironucleus muris* using transmission electron microscopy. Int. J. Parasitol 24 (5), 695–703. [PubMed: 7928072]

Palm JE, Weiland ME, Griffiths WJ, Ljungstrom I, Svard SG, 2003. Identification of immunoreactive proteins during acute human giardiasis. J. Infect. Dis 187 (12), 1849–1859. [PubMed: 12792861]

Palm D, Weiland M, McArthur AG, Winiecka-Krusnell J, Cipriano MJ, Birkeland SR, Pacocha SE, Davids B, Gillin F, Linder E, Svard S, 2005. Developmental changes in the adhesive disk during *Giardia* differentiation. Mol. Biochem. Parasitol 141 (2), 199–207. [PubMed: 15850703]

Paredez AR, Assaf ZJ, Sept D, Timofejeva L, Dawson SC, Wang CJ, Cande WZ, 2011. An actin cytoskeleton with evolutionarily conserved functions in the absence of canonical actin-binding proteins. Proc. Natl. Acad. Sci. U. S. A 108 (15), 6151–6156. [PubMed: 21444821]

Pazour GJ, Witman GB, 2003. The vertebrate primary cilium is a sensory organelle. Curr. Opin. Cell Biol 15 (1), 105–110. [PubMed: 12517711]

Pazour GJ, Agrin N, Leszyk J, Witman GB, 2005. Proteomic analysis of a eukaryotic cilium. J. Cell Biol 170 (1), 103–113. [PubMed: 15998802]

Peattie DA, 1990. The giardins of *Giardia lamblia*: genes and proteins with promise. Parasitol. Today 6 (2), 52–56. [PubMed: 15463296]

Pellegrini F, Budman DR, 2005. Review: tubulin function, action of antitubulin drugs, and new drug development. Cancer Investig. 23 (3), 264–273. [PubMed: 15948296]

Pfannenschmid F, Wimmer VC, Rios RM, Geimer S, Krockel U, Leiherer A, Haller K, Nemcova Y, Mages W, 2003. *Chlamydomonas* DIP13 and human NA14: a new class of proteins associated with microtubule structures is involved in cell division. J. Cell Sci 116 (Pt. 8), 1449–1462. [PubMed: 12640030]

Piva B, Benchimol M, 2004. The median body of *Giardia lamblia*: an ultrastructural study. Biol. Cell 96 (9), 735–746. [PubMed: 15567529]

Poxleitner MK, Carpenter ML, Mancuso JJ., Wang CJ, Dawson SC, Cande WZ, 2008. Evidence for karyogamy and exchange of genetic material in the binucleate intestinal parasite *Giardia intestinalis*. Science 319 (5869), 1530–1533. [PubMed: 18339940]

Preisner H, Karin EL, Poschmann G, Stuhler K, Pupko T, Gould SB, 2016. The cytoskeleton of parabasalian parasites comprises proteins that share properties common to intermediate filament proteins. Protist 167 (6), 526–543. [PubMed: 27744090]

Ren B, Gupta N, 2017. Taming parasites by tailoring them. Front. Cell. Infect. Microbiol7, 292. [PubMed: 28730142]

Rescher U, Gerke V, 2004. Annexins—unique membrane binding proteins with diverse functions. J. Cell Sci 117 (Pt. 13), 2631–2639. [PubMed: 15169834]

Rosenbaum JL, Witman GB, 2002. Intraflagellar transport. Nat. Rev. Mol. Cell Biol 3 (11), 813–825. [PubMed: 12415299]

Roxstrom-Lindquist K, Palm D, Reiner D, Ringqvist E, Svard SG, 2006. Giardia immunity—an update. Trends Parasitol. 22 (1), 26–31. [PubMed: 16303332]

Russell JJ, Theriot JA, Sood P, Marshall WF, Landweber LF, Fritz-Laylin L, Polka JK, Oliferenko S, Gerbich T, Gladfelter A, Umen J, Bezanilla M, Lancaster MA, He S, Gibson MC, Goldstein B, Tanaka EM, Hu CK, Brunet A, 2017. Non-model model organisms. BMC Biol. 15 (1), 55. [PubMed: 28662661]

Sagolla MS, Dawson SC, Mancuso JJ, Cande WZ, 2006. Three-dimensional analysis of mitosis and cytokinesis in the binucleate parasite *Giardia intestinalis*. J. Cell Sci 119 (Pt. 23), 4889–4900. [PubMed: 17105767]

Scholey JM, 2003. Intraflagellar transport. Annu. Rev. Cell Dev. Biol 19, 423–443. [PubMed: 14570576]

Schwartz CL, Heumann JM, Dawson SC, Hoenger A, 2012. A detailed, hierarchical study of *Giardia lamblia's* ventral disc reveals novel microtubule-associated protein complexes. PLoS One 7 (9), e43783. [PubMed: 22984443]

Song Y, Brady ST, 2015. Post-translational modifications of tubulin: pathways to functional diversity of microtubules. Trends Cell Biol 25 (3), 125–136. [PubMed: 25468068]

Sousa M, Concalves CA, Bairos VA, Poiares-Da-Silva J, 2001. Adherence of *Giardia lamblia* trophozoites to Int-407 human intestinal cells. Clin. Diagn. Lab. Immunol 8, 258–265. [PubMed: 11238205]

Szkodowska A, Muller MC, Linke C, Scholze H, 2002. Annexin XXI (ANX21) of *Giardia lamblia* has sequence motifs uniquely sdhared by giardial annexins and is specifically localized in the flagella. J. Biol. Chem 277 (28), 25703–25706. [PubMed: 12006598]

Tumova P, Kulda J, Nohynkova E, 2007. Cell division of *Giardia intestinalis*: assembly and disassembly of the adhesive disc, and the cytokinesis. Cell Motil. Cytoskeleton 64 (4), 288–298. [PubMed: 17205565]

Vahrmann A, Saric M, Scholze H, Koebsch I, 2008. alpha14-Giardin (annexin E1) is associated with tubulin in trophozoites of *Giardia lamblia* and forms local slubs in the flagella. Parasitol. Res 102 (2), 321–326. [PubMed: 17938962]

Vicente JJ, Cande WZ, 2014. Mad2, Bub3, and Mps1 regulate chromosome segregation and mitotic synchrony in *Giardia intestinalis*, a binucleate protist lacking an anaphase-promoting complex. Mol. Biol. Cell 25 (18), 2774–2787. [PubMed: 25057014]

Wei CJ, Tian XF, Adam RD, Lu SQ, 2010. *Giardia lamblia*: intracellular localization of alpha8-giardin. Exp. Parasitol 126 (4), 489–496. [PubMed: 20515687]

Weiland ME, Palm JE, Griffiths WJ, McCaffery JM, Svard SG, 2003. Characterisation of alpha-1 giardin: an immunodominant *Giardia lamblia* annexin with glycosaminoglycan-binding activity. Int. J. Parasitol 33 (12), 1341–1351. [PubMed: 14527517]

Weiland ME, McArthur AG, Morrison HG, Sogin ML, Svard SG, 2005. Annexin-like alpha giardins: a new cytoskeletal gene family in *Giardia lamblia*. Int. J. Parasitol 35 (6), 617–626. [PubMed: 15862575]

Weisbrich A, Honnappa S, Jaussi R, Okhrimenko O, Frey D, Jelesarov I, Akhmanova A, Steinmetz MO, 2007. Structure-function relationship of CAP-Gly domains. Nat. Struct. Mol. Biol 14 (10), 959–967. [PubMed: 17828277]

Wickstead B, Gull K, 2006. A “holistic” kinesin phylogeny reveals new kinesin families and predicts protein functions. Mol. Biol. Cell 17 (4), 1734–1743. [PubMed: 16481395]

Wickstead B, Gull K, 2007. Dyneins across eukaryotes: a comparative genomic analysis. Traffic 8 (12), 1708–1721. [PubMed: 17897317]

Woessner DJ, Dawson SC, 2012. The Giardia median body protein is a ventral disc protein that is critical for maintaining a domed disc conformation during attachment. Eukaryot. Cell 11 (3), 292–301. [PubMed: 22247266]

Wu S, Pan W, Shi X, Abdullahi AY, Wang Z, Yu X, Jiang B, Li K, Xu C, Li G, 2016. Immunolocalization of alpha18- and alpha12-giardin in *Giardia lamblia* trophozoites. Parasitol. Res 115 (11), 4183–4187. [PubMed: 27465564]

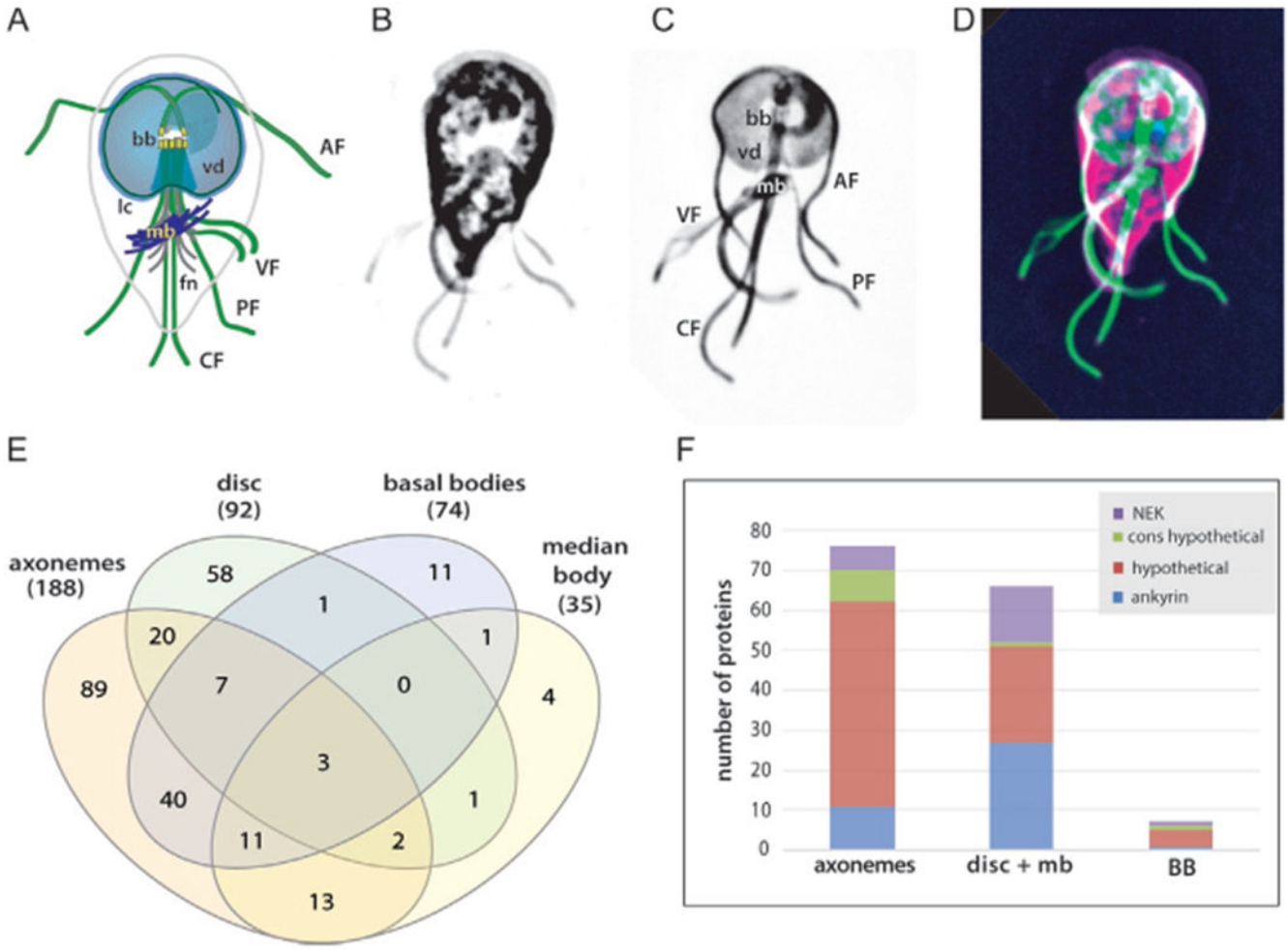

Fig. 1.

Many cytoskeletal proteins associated with microtubule organelles in *Giardia* lack MT binding motifs. The schematic of the *Giardia* trophozoite cytoskeleton (A) indicates the ventral disc (vd) and lateral crest (lc), the four flagellar pairs (AF, anterior; PF, posteriolateral; VF, ventral; CF, caudal) and basal bodies (bb), as well as the median body (mb) and funis (fn). The teardrop cell shape is visible in panel B (CellMask membrane stain) and the primary MT organelles are also highlighted in an N-terminally tagged mNeonGreen (mNG) beta-tubulin strain (C). The merged image in panel D highlights the MT organelles (mNG-beta-tubulin, green), (CellMask, magenta) with DAPI (blue) to stain the nuclei. Over 300 cytoskeletal proteins have been identified bioinformatically or localized to one or more MT arrays (panel E and Tables 1–3). Many *Giardia* cytoskeleton-associated proteins lack homology or MT binding motifs (hypothetical or conserved hypothetical) or simply have conserved ankyrin repeat domains or are NIMA (NEK) kinases, yet different MT organelles (axonemes, basal bodies, disc, median body) have different numbers of these overrepresented categories (F).

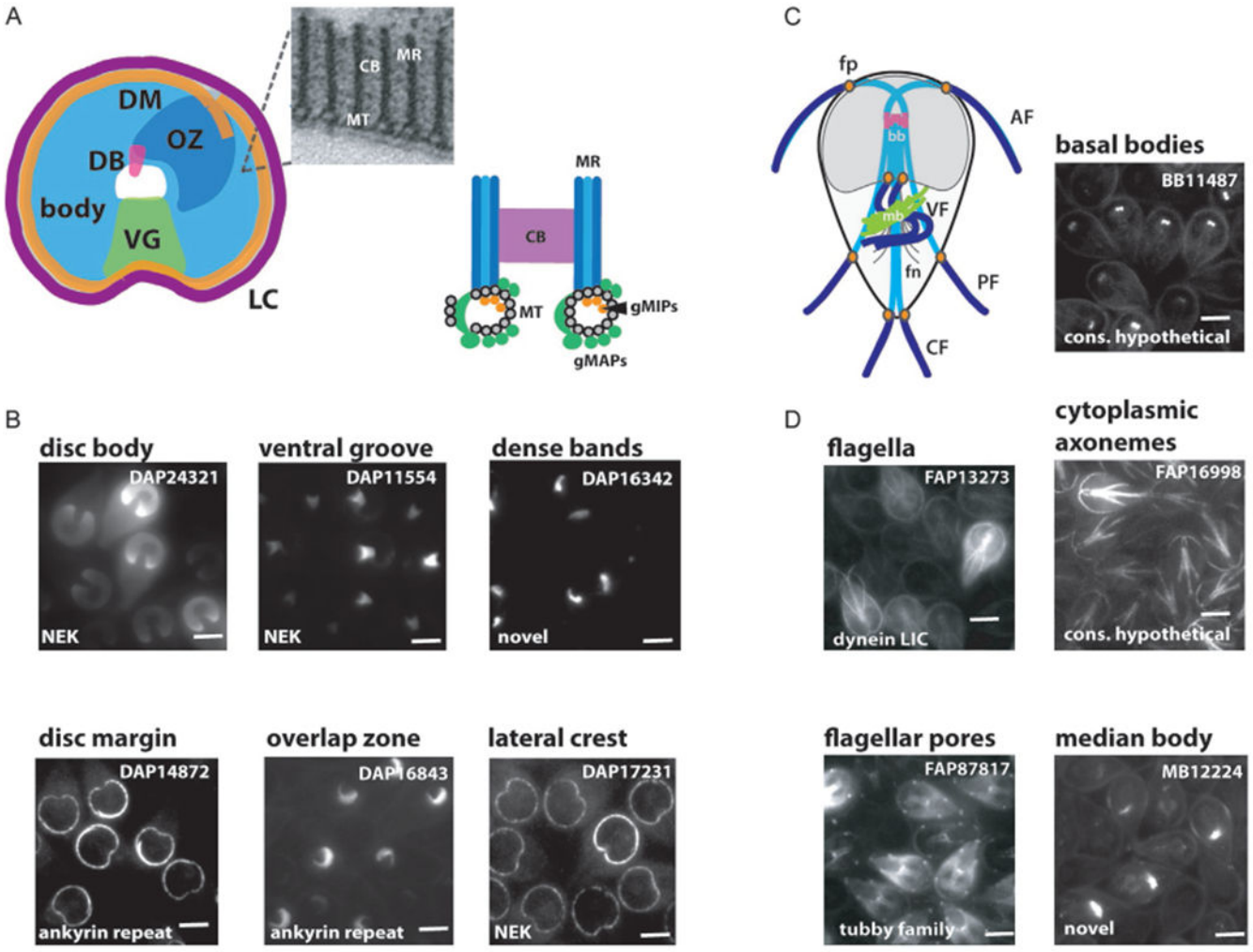

Fig. 2.

Localization of both conserved and novel cytoskeletal proteins to all MT organelles. More than 90 disc-associated proteins (DAPs) have been identified and localized to the complex ventral disc architecture, which includes the abundant microribbon (MR)/crossbridge (CB) complexes associated with the disc MTs (see schematic in A). As illustrated by representative images of GFP-tagged DAPs in panel B, some localize to the disc body or to one or more structurally defined regions of the disc (e.g., VG, ventral groove; DM, disc margin; OZ, overlap zone; DB, dense bands; LC, lateral crest). *Giardia* axonemes have specific cytoplasmic (light blue) and membrane-bound regions (dark blue), and axonemes exit the cell body at flagellar pores (see orange in schematic in C). Representative GFP-tagged cytoskeletal proteins illustrate that many proteins localize specifically to the basal bodies (bb), the median body (mb), or either to the entire length of some or all the flagella, or only to the cytoplasmic portions of the axonemes or to the flagellar pores (fp).

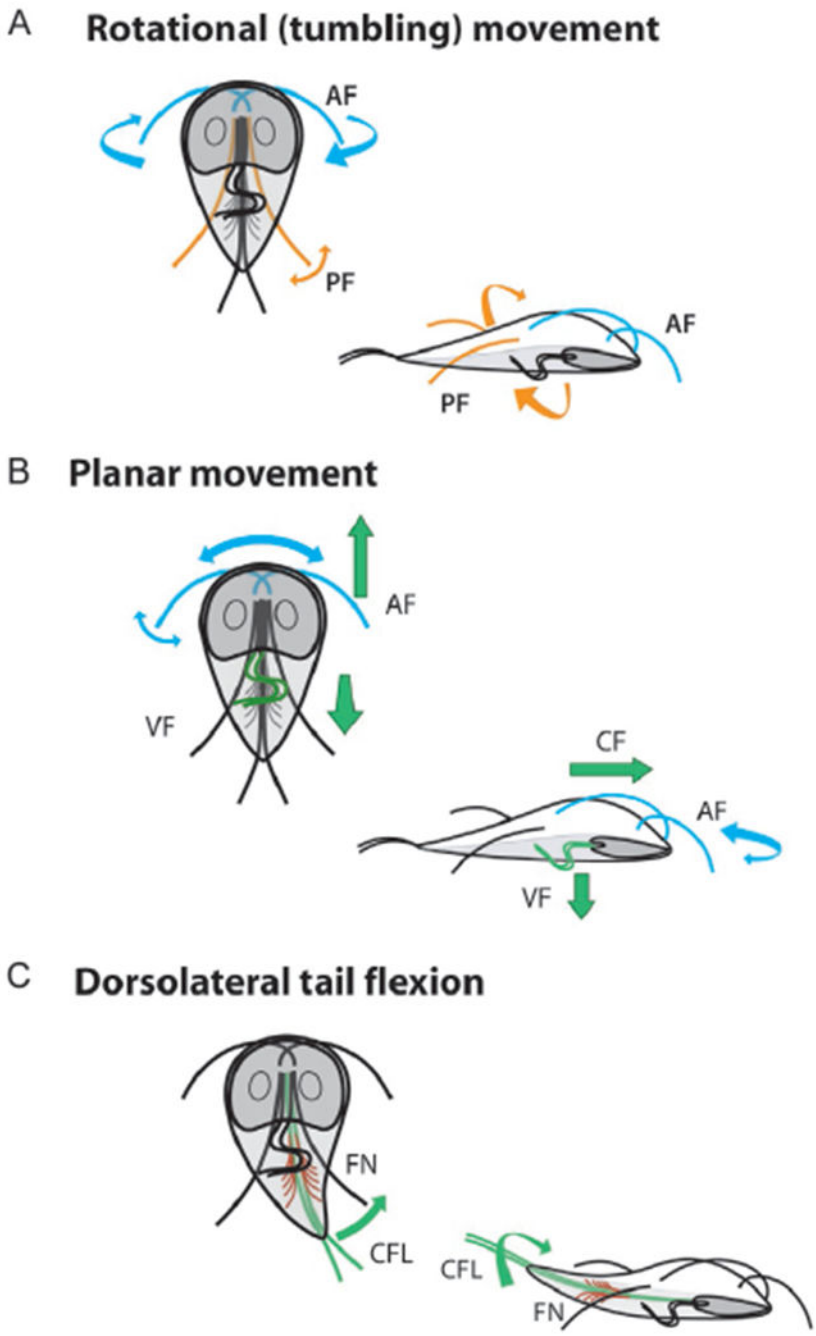

Fig. 3.

Complex motility in the multiflagellated trophozoite. During rapid, rotational swimming (A), undulating movements of the caudal region propel the trophozoite forward and are accompanied by paddle-like beating of the anterior and posteriolateral flagella. Prior to attachment, motion slows, and swimming becomes stable and planar (B), with the ventral disc oriented towards the attachment surface. Ventral flagellar beating may produce a force that drives the disc downward. Dorsolateral tail flexion (C) has been attributed to the funis or caudal complex and may promote detachment.

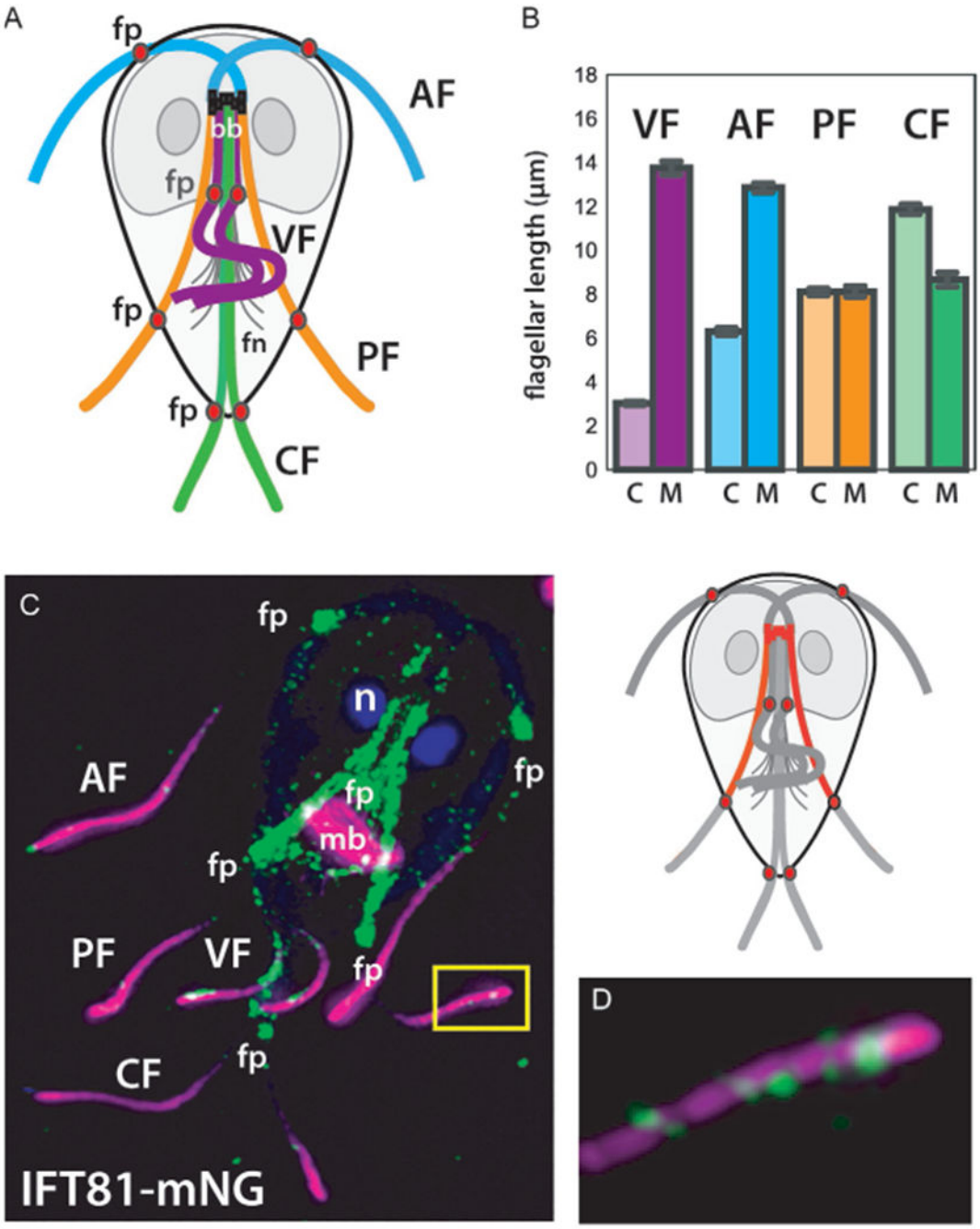

Fig. 4.

Flagellar structure and assembly of the eight flagella. Each of the eight axonemes are nucleated by basal bodies located in the cytoplasm between the two nuclei (see schematic in A). Each axoneme also extends through the cytoplasm and is compartmentalized into a membrane-bound flagellum at the flagellar pores (fp). Yet each flagellar pair (AF, anterior; VF, ventral; CF, caudal; PF, posteriolateral) has different lengths in both the cytoplasmic and the membrane-bound regions (B). Flagellar assembly and length maintenance are generally achieved by intraflagellar transport (IFT) powered by MT motors. In *Giardia*, IFT particles

assemble on cytoplasmic portions, accumulate at flagellar pores (fp) and are actively trafficked by IFT on membrane-bound portions as illustrated (see C, D) using a marker of IFT trains (mNG-tagged IFT81, green; MTs, magenta).

Table 1

Inventory of conserved cytoskeletal proteins associated with the MT cytoskeleton.

GiardiaDB	Protein name	Protein family	PFAM	BB	AX	DSC	MB	FN	SN	MS	Other localization	Evidence	References
Alpha- and beta-tubulins													
GL50803_103676	Alpha-tubulin 1	Tubulin	PF00091	X	X	X	X	X	X	X		HOM, IFA	Campanati et al. (2003)
GL50803_112079	Alpha-tubulin 2	Tubulin	PF00091	X	X	X	X	X	X	X		HOM, IFA	Campanati et al. (2003)
GL50803_101291	Beta-tubulin 1	Tubulin	PF00091	X	X	X	X	X	X	X		HOM, IFA, GFP, mNG	Campanati et al. (2003) and Hardin et al. (2017)
GL50803_136021	Beta-tubulin 2	Tubulin	PF00091	X	X	X	X	X	X	X		HOM, IFA	Campanati et al. (2003)
GL50803_136020	Beta-tubulin 3	Tubulin	PF00091	X	X	X	X	X	X	X		HOM, IFA	Campanati et al. (2003)
Basal body/gamma-TuRC complex													
GL50803_6744	Centrin	Centrin	PF13499	X								HOM, IFA	Belhadri (1995)
GL50803_104685	Centrin	Centrin	PF13499	X								HOM, IFA, GFP	Meng et al. (1996), Dawsonlab (GiardiaDB)
GL50803_5462	Delta-tubulin	Tubulin	PF00091								Cytoplasm	HOM, GFP	Dawsonlab (GiardiaDB)
GL50803_6336	Epsilon-tubulin	Tubulin	PF00091								Cytoplasm	HOM, GFP	Dawsonlab (GiardiaDB)
GL50803_114218	Gamma-tubulin	Tubulin	PF00091	X							Cytoplasm	HOM, IFA, GFP	Dawsonlab (GiardiaDB), Lauwaet et al. (2011)
GL50803_17429	GCP2	Spc97_Spc98	PF04130								n.d.	HOM	Morrison et al. (2007)
GL50803_12057	GCP3	Spc97_Spc98	PF04130	X	X		X					HOM, GFP	Dawsonlab (GiardiaDB)
GL50803_4689	Hypothetical protein	None	None	X	X							EPI	Lauwaet et al. (2011)
GL50803_4692	Hypothetical protein	None	None	X								EPI	Lauwaet et al. (2011)
GL50803_104150	Polo-like kinase, PLK	Ser/Thr kinase domain, POLO box domain	PF00659	X								EPI	Lauwaet et al. (2011)
GL50803_16220	Ankyrin repeat protein	Ankyrin repeat domain	PF12796	X							Plasma membrane, cytoplasm	GFP	Dawsonlab (GiardiaDB)
GL50803_5333	Calmodulin	EF-hand domain	PF13499	X							Plasma membrane	GFP	Dawsonlab (GiardiaDB)
GL50803_11487	Conserved hypothetical protein	None	None	X								GFP	Dawsonlab (GiardiaDB)

GiardiaDB	Protein name	Protein family	PFAM	BB	AX	DSC	MB	FN	SN	MS	Other localization	Evidence	References
GL50803_16192	Hypothetical protein	None	None	X		X						GFP	Dawsonlab (GiardiaDB)
GL50803_15193	Hypothetical protein	None	None	X								IFA, GFP	Lauwaet et al. (2011), Dawsonlab (GiardiaDB)
GL50803_9665	Nek kinase GK272	NEK	PF00069	X							Plasma membrane	GFP	Dawsonlab (GiardiaDB)
MT dynamics/regulators													
GL50803_14373	Dynamin	Dynamin	PF00350								Plasma membrane	GFP	Dawsonlab (GiardiaDB)
GL50803_14048	EB1	EB1-like C-terminal motif	PF03271		X		X			X	Nuclear membrane	GFP	Dawson et al. (2007)
GL50803_15368	Katanin (p60)	AAA ATPase family	PF00004	X	X		X					GFP	Dawsonlab (GiardiaDB)
GL50803_11953	Katanin (p80)	WD-40 repeat protein	PF00400								n.d.	HOM	Morrison et al. (2007)
GL50803_15054	Kelch repeat domain containing protein	Kelch2 repeat domain	PF0646		X							GFP	Dawsonlab (GiardiaDB)
GL50803_94322	Spastin	AAA ATPase family	PF00004	X								GFP	Dawsonlab (GiardiaDB)
GL50803_91480	stu2	Stu2 family	None								n.d.	HOM	Morrison et al. (2007)
GL50803_16893	Tip elongation aberrant protein 1	Kelch2 repeat domain	PF0646		X							GFP	Dawsonlab (GiardiaDB)
GL50803_16535	Tubulin-specific chaperone E	CAP-GLY	PF01302								n.d.	HOM	Morrison et al. (2007)
GL50803_96399	xmap215	XMAP215 family	None								n.d.	HOM	Morrison et al. (2007)
Tubulin modification													
GL50803_95661	Tubulin tyrosine ligase	Tubulin tyrosine ligase	PF03133		X							HOM, GFP	Dawsonlab (GiardiaDB)
GL50803_10801	Tubulin tyrosine ligase	Tubulin tyrosine ligase	PF03133								Cytoplasm	HOM, GFP	Dawsonlab (GiardiaDB)
GL50803_8456	Tubulin tyrosine ligase	Tubulin tyrosine ligase	PF03133								Cytoplasm	HOM, GFP	Dawsonlab (GiardiaDB)
GL50803_10382	Tubulin tyrosine ligase	Tubulin tyrosine ligase	PF03133								n.d.	HOM	Morrison et al. (2007)
GL50803_14498	Tubulin tyrosine ligase	Tubulin tyrosine ligase	PF03133								n.d.	HOM	Morrison et al. (2007)
GL50803_8592	Tubulin tyrosine ligase	Tubulin tyrosine ligase	PF03133								n.d.	HOM	Morrison et al. (2007)

GiardiaDB	Protein name	Protein family	PFAM	BB	AX	DSC	MB	FN	SN	MS	Other localization	Evidence	References
GL50803_9272	Tubulin tyrosine ligase	Tubulin tyrosine ligase	PF03133								n.d.	HOM	Morrison et al. (2007)
Microtubule motors													
Axonemal dyneins													
GL50803_100906	IAD-1alpha	IAD-1alpha dynein heavy chain (DHC) family	PF03028		X						n.d.	HOM	Wickstead and Gull (2007)
GL50803_94440	IAD-1beta	IAD-1beta dynein heavy chain (DHC) family	PF03028		X						n.d.	HOM	Wickstead and Gull (2007)
GL50803_40496	IAD-4	IAD-4 dynein heavy chain (DHC) family	PF03028		X						n.d.	HOM	Wickstead and Gull (2007)
GL50803_37985	IAD-4	IAD-4 dynein heavy chain (DHC) family, partial	PF03028		X						n.d.	HOM	Wickstead and Gull (2007)
GL50803_111950	IAD-5	IAD-5 dynein heavy chain (DHC) family	PF03028		X						n.d.	HOM	Wickstead and Gull (2007)
GL50803_17265	OAD-alpha	OAD-alpha dynein heavy chain (DHC) family	PF03028		X						n.d.	HOM	Wickstead and Gull (2007)
GL50803_17243	OAD-beta	OAD-beta dynein heavy chain (DHC) family	PF03028		X						n.d.	HOM	Wickstead and Gull (2007)
Other dynein heavy chains													
GL50803_17478	cytoDHC	CytoDHC cytoplasmic dynein heavy chain family	PF03028								n.d.	HOM	Wickstead and Gull (2007)
GL50803_93736	cytoDHC-1b	CytoDHC cytoplasmic dynein heavy chain family	PF03028								n.d.	HOM	Wickstead and Gull (2007)
GL50803_29256	DHC 1	Axonemal dynein heavy chain, partial	PF03028								n.d.	HOM	Wickstead and Gull (2007)
GL50803_101138	DHC 2	Dynein heavy chain (DHC) family	PF03028								n.d.	HOM	Wickstead and Gull (2007)
GL50803_103059	DHC 3	Dynein heavy chain (DHC) family	PF03028								n.d.	HOM	Wickstead and Gull (2007)
GL50803_10538	DHC 4	Dynein heavy chain (DHC) family	PF03028								n.d.	HOM	Wickstead and Gull (2007)
GL50803_16804	DHC 5	Dynein heavy chain (DHC) family	PF03028								n.d.	HOM	Wickstead and Gull (2007)

GiardiaDB	Protein name	Protein family	PFAM	BB	AX	DSC	MB	FN	SN	MS	Other localization	Evidence	References
GL50803_8172	DHC 6	Dynein heavy chain (DHC) family, partial	PF03028								n.d.	HOM	Wickstead and Gull (2007)
Dynein regulatory complex													
GL50803_16540	PF2	Dynein regulatory complex (DRC); trypanin	PD936484								n.d.	HOM	Morrison et al. (2007)
Dynein intermediate chains													
GL50803_10254	IC138	Dynein intermediate chain (DIC) family	PF05783								n.d.	HOM	Wickstead and Gull (2007)
GL50803_6939	IC70	Dynein intermediate chain (DIC) family	PF05783								n.d.	HOM	Wickstead and Gull (2007)
GL50803_33218	IC78	Dynein intermediate chain (DIC) family, ODA-IC1	PF05783								n.d.	HOM	Wickstead and Gull (2007)
Dynein light chains													
GL50803_17371	DYNLT1 (Tctex1/ LC9)	Tctex-1 family	PF03645								n.d.	HOM	Wickstead and Gull (2007)
GL50803_4236	DYNLT1 (Tctex1/ LC9)	Tctex-1 family	PF03645								n.d.	HOM	Wickstead and Gull (2007)
GL50803_13575	DYNLT2 (Tctex2/ LC19)	Tctex-1 family	PF01221								n.d.	HOM	Wickstead and Gull (2007)
GL50803_4463	LC1	Dynein light chain (DLC) family	PF01221								n.d.	HOM	Wickstead and Gull (2007)
GL50803_27308	LC4	Dynein light chain (DLC) family	PF01221								Plasma membrane	GFP	Dawsonlab (GiardiaDB)
GL50803_7578	LC5	Dynein light chain (DLC) family	PF01221								Plasma membrane	GFP	Dawsonlab (GiardiaDB)
GL50803_9848	LC8	Dynein light chain (DLC) family	PF03645	X	X							GFP	Dawsonlab (GiardiaDB)
GL50803_14270	Roadblock/LC7	Roadblock-related dynein light chain	PD03259		X							GFP	Dawsonlab (GiardiaDB)
GL50803_15124	Roadblock/LC7	Roadblock/LC7 domain family	PD03259								n.d.	HOM	Wickstead and Gull (2007)
GL50803_15606	Tctex-I	Tctex-1 family	PF03645								n.d.	HOM	Wickstead and Gull (2007)
Dynein light intermediate chain													

GiardiaDB	Protein name	Protein family	PFAM	BB	AX	DSC	MB	FN	SN	MS	Other localization	Evidence	References
GL50803_13273	Axonemal DLIC	Axonemal dynein light chain family, p28	PF10211		X							GFP	Dawsonlab (GiardiaDB)
Kinesins													
GL50803_11177	KLC	Kinesin light chain	SSF81901	X	X							HOM, GFP	Dawsonlab (GiardiaDB)
GL50803_13825	GiKIN1	Kinesin-1	PF00225								n.d.	HOM	Wickstead and Gull (2006)
GL50803_17333	GiKIN2a	Kinesin-2	PF00225	X	X							HOM, GFP	McInally et al. (2020)
GL50803_16456	GiKIN2b	Kinesin-2	PF00225	X	X							HOM, GFP	McInally et al. (2020)
GL50803_6262	GiKIN3a	Kinesin-3	PF00225								n.d.	HOM	Wickstead and Gull (2006)
GL50803_102101	GiKIN3b	Kinesin-3	PF00225								n.d.	HOM	Wickstead and Gull (2006)
GL50803_112846	GiKIN3c	Kinesin-3	PF00225								n.d.	HOM	Wickstead and Gull (2006)
GL50803_16650	GiKIN4	Kinesin-4	PF00225								n.d.	HOM	Wickstead and Gull (2006)
GL50803_16425	GiKIN5	Kinesin-5	PF00225								n.d.	HOM	Wickstead and Gull (2006)
GL50803_102455	GiKIN6a	Kinesin-6	PF00225	X	X	X	X					HOM, GFP	Dawsonlab (GiardiaDB)
GL50803_15134	GiKIN6b	Kinesin-6	PF00225								n.d.	HOM	Wickstead and Gull (2006)
GL50803_15962	GiKIN7	Kinesin-7	PF00225								n.d.	HOM	Wickstead and Gull (2006)
GL50803_4371	GiKIN8	Kinesin-8	PF00225								Nuclei, nucleolus	GFP	Dawsonlab (GiardiaDB)
GL50803_10137	GiKIN9a	Kinesin-9	PF00225								n.d.	HOM	Wickstead and Gull (2006)
GL50803_6404	GiKIN9b	Kinesin-9	PF00225								n.d.	HOM	Wickstead and Gull (2006)
GL50803_16945	GiKIN13	Kinesin-13	PF00225		X			X				GFP	Dawson et al. (2007)
GL50803_8886	GiKIN14a	Kinesin-14	PF00225								nuclei	GFP	Dawsonlab (GiardiaDB)
GL50803_13797	GiKIN14b	Kinesin-14	PF00225								n.d.	HOM	Wickstead and Gull (2006)
GL50803_7874	GiKIN16a	Kinesin-16	PF00225								n.d.	HOM	Wickstead and Gull (2006)

GiardiaDB	Protein name	Protein family	PFAM	BB	AX	DSC	MB	FN	SN	MS	Other localization	Evidence	References
GL50803_16161	GiKIN16b	Kinesin-16	PF00225								n.d.	HOM	Wickstead and Gull (2006)
GL50803_16224	GiKIN20	Orphan kinesin	PF00225								n.d.	HOM	Wickstead and Gull (2006)
GL50803_17264	GiKIN21	Orphan kinesin	PF00225								n.d.	HOM	Wickstead and Gull (2006)
GL50803_14070	GiKIN22	Orphan kinesin	PF00225		X							GFP	Dawsonlab (GiardiaDB)
GL50803_112729	GiKIN23	Orphan kinesin	PF00225								n.d.	HOM	Wickstead and Gull (2006)
GL50803_11442	GiKIN24	Orphan kinesin	PF00225								n.d.	HOM	Wickstead and Gull (2006)

More than 90 conserved cytoskeleton-associated proteins are encoded by the *Giardia lamblia* (ATCC 50803) genome (Morrison et al., 2007), including tubulins and tubulin modifying enzymes, regulators of MT dynamics, basal body and BBsomes, and microtubule motors. Conserved cytoskeletal proteins have been identified based on homology to known cytoskeleton-associated proteins in other organisms (HOM) as well as by subcellular localization using heterologous antibodies (IFA), epitope-tagging (EPI), or fluorescent tags (GFP, mNG) to the basal bodies (BB), axonemes (AX), disc (DSC), median body (MB), funis (FN), supernumerary MTs (SN) or mitotic spindles (MS).

Table 2

Inventory of conserved and novel ventral disc and median body proteins.

GiardiaDB	Protein name	Protein family	PFAM	BB	AX	DSC	MB	FN	SN	MS	Other localization	Evidence	References
Disc-associated proteins (*DAPs*)													
GL50803_15101	Alpha17-giardin	Annexin	PF00191		X	X						HOM, EPI	Weiland et al. (2005)
GL50803_7796	Alpha2-giardin	Annexin	PF00191		X	X						GFP	House et al. (2011)
GL50803_11683	Alpha3-giardin	Annexin	PF00191			X						HOM, EPI	Weiland et al. (2005)
GL50803_7797	Alpha5-giardin	Annexin	PF00191		X	X						HOM, EPI	Weiland et al. (2005)
GL50803_11649	Alpha8-giardin	Annexin	PF00191		X							IFA	Wei et al. (2010)
GL50803_17097	Ankyrin repeat protein	Ankyrin repeat domain	PF12796		X	X						GFP	Nosala et al. (2019)
GL50803_14800	Ankyrin repeat protein	Ankyrin repeat domain	PF12796		X	X					Marginal plates	GFP	Nosala et al. (2019)
GL50803_13590	Ankyrin repeat protein	Ankyrin repeat domain	PF12796		X	X						GFP	Nosala et al. (2019)
GL50803_137684	Ankyrin repeat protein	Ankyrin repeat domain	PF12796		X	X						GFP	Nosala et al. (2019)
GL50803_14681	Ankyrin repeat protein	Ankyrin repeat domain	PF12796		X	X						GFP	Nosala et al. (2019)
GL50803_3760	Ankyrin repeat protein	Ankyrin repeat domain	PF12796			X					Cytoplasm	GFP	Nosala et al. (2019)
GL50803_10219	Ankyrin repeat protein	Ankyrin repeat domain	PF12796			X						GFP	Nosala et al. (2019)
GL50803_103807	Ankyrin repeat protein	Ankyrin repeat domain	PF12796			X						GFP	Nosala et al. (2019)
GL50803_103810	Ankyrin repeat protein	Ankyrin repeat domain	PF12796			X						GFP	Nosala et al. (2019)
GL50803_112557	Ankyrin repeat protein	Ankyrin repeat domain	PF12796			X						GFP	Nosala et al. (2019)
GL50803_12139	Ankyrin repeat protein	Ankyrin repeat domain	PF12796			X						GFP	Nosala et al. (2019)
GL50803_13766	Ankyrin repeat protein	Ankyrin repeat domain	PF12796			X						GFP	Nosala et al. (2019)
GL50803_14859	Ankyrin repeat protein	Ankyrin repeat domain	PF12796			X						GFP	Nosala et al. (2019)
GL50803_14872	Ankyrin repeat protein	Ankyrin repeat domain	PF12796			X						GFP	Nosala et al. (2019)
GL50803_15576	Ankyrin repeat protein	Ankyrin repeat domain	PF12796			X						GFP	Nosala et al. (2019)
GL50803_16843	Ankyrin repeat protein	Ankyrin repeat domain	PF12796			X						GFP	Nosala et al. (2019)
GL50803_17053	Ankyrin repeat protein	Ankyrin repeat domain	PF12796			X						GFP	Nosala et al. (2019)
GL50803_17096	Ankyrin repeat protein	Ankyrin repeat domain	PF12796			X						GFP	Nosala et al. (2019)
GL50803_17551	Ankyrin repeat protein	Ankyrin repeat domain	PF12796			X						GFP	Nosala et al. (2019)
GL50803_23492	Ankyrin repeat protein	Ankyrin repeat domain	PF12796			X						GFP	Nosala et al. (2019)

GiardiaDB	Protein name	Protein family	PFAM	BB	AX	DSC	MB	FN	SN	MS	Other localization	Evidence	References
GL50803_24194	Ankyrin repeat protein	Ankyrin repeat domain	PF12796			X						GFP	Nosala et al. (2019)
GL50803_40016	Ankyrin repeat protein	Ankyrin repeat domain	PF12796			X						GFP	Nosala et al. (2019)
GL50803_5188	Ankyrin repeat protein	Ankyrin repeat domain	PF12796			X						GFP	Nosala et al. (2019)
GL50803_7268	Ankyrin repeat protein	Ankyrin repeat domain	PF12796			X						GFP	Nosala et al. (2019)
GL50803_7414	Ankyrin repeat protein	Ankyrin repeat domain	PF12796			X						GFP	Nosala et al. (2019)
GL50803_8850	Ankyrin repeat protein	Ankyrin repeat domain	PF12796			X						GFP	Nosala et al. (2019)
GL50803_9515	Ankyrin repeat protein	Ankyrin repeat domain	PF12796			X						GFP	Nosala et al. (2019)
GL50803_5358	Aurora kinase	Aurora kinase	PF00069	X	X	X	X				Nuclei	EPI	Davids et al. (2008)
GL50803_4812	Beta-giardin	SF-assemblin	PF06705			X						IFA	Baker et al. (1988)
GL50803_86676	Delta-giardin	SF-assemblin	PF06705			X						IFA, GFP	Nosala et al. (2019)
GL50803_16263	DIP13	DIP13	None		X	X						GFP	Nosala et al. (2019)
GL50803_5568	DUF866 domain protein	DUF866	PF05907	X	X	X						GFP	Nosala et al. (2019)
GL50803_3256	Epsin	ENTH	PF01417			X						EPI	Ebneter and Hehl (2014)
GL50803_17563	ERK1 kinase	CMGC MAPK	PF00069	X	X	X	X					EPI	Ellis et al. (2003)
GL50803_41512	Flagella associated protein Rib72	DUF1126	PF06565	X	X	X						EPI, GFP	Nosala et al. (2019) and Lauwaet et al. (2011)
GL50803_17230	Gamma-giardin	None	None			X						IFA, EPI	Nohria et al. (1992) and Kim and Park (2019)
GL50803_102455	GiKIN6a	Kinesin-6	PF00225		X	X						GFP	Nosala et al. (2019)
GL50803_101326	Hypothetical protein	None	None		X	X						GFP	Nosala et al. (2019)
GL50803_16935	Hypothetical protein	None	None		X	X						GFP	Nosala et al. (2019)
GL50803_24537	Hypothetical protein	None	None		X	X						GFP	Nosala et al. (2019)
GL50803_2556	Hypothetical protein	None	None		X	X						GFP	Nosala et al. (2019)
GL50803_33866	Hypothetical protein	None	None		X	X						GFP	Nosala et al. (2019)
GL50803_6709	Hypothetical protein	None	None		X	X						GFP	Nosala et al. (2019)
GL50803_7520	Hypothetical protein	None	None		X	X						GFP	Nosala et al. (2019)
GL50803_86815	Hypothetical protein	None	None			X	X				Cytoplasm	GFP	Nosala et al. (2019)
GL50803_4239	Hypothetical protein	None	None			X					Cytoplasm	GFP	Nosala et al. (2019)
GL50803_6171	Hypothetical protein	None	None			X					Cytoplasm	GFP	Nosala et al. (2019)

GiardiaDB	Protein name	Protein family	PFAM	BB	AX	DSC	MB	FN	SN	MS	Other localization	Evidence	References
GL50803_20688	Hypothetical protein	None	None			X						GFP	Dawsonlab (GiardiaDB)
GL50803_4852	Hypothetical protein	None	None			X						EPI	Lauwaet et al. (2011)
GL50803_10181	Hypothetical protein	None	None			X						GFP	Nosala et al. (2019)
GL50803_10232	Hypothetical protein	None	None			X						GFP	Nosala et al. (2019)
GL50803_10524	Hypothetical protein	None	None			X						GFP	Nosala et al. (2019)
GL50803_13651	Hypothetical protein	None	None			X						GFP	Nosala et al. (2019)
GL50803_15499	Hypothetical protein	None	None			X						GFP	Nosala et al. (2019)
GL50803_15918	Hypothetical protein	None	None			X						GFP	Nosala et al. (2019)
GL50803_16342	Hypothetical protein	None	None			X						GFP	Nosala et al. (2019)
GL50803_17412	Hypothetical protein	None	None			X						GFP	Nosala et al. (2019)
GL50803_3934	Hypothetical protein	None	None			X						GFP	Nosala et al. (2019)
GL50803_5883	Hypothetical protein	None	None			X						GFP	Nosala et al. (2019)
GL50803_6751	Hypothetical protein	None	None			X						GFP	Nosala et al. (2019)
GL50803_8726	Hypothetical protein	None	None			X						GFP	Nosala et al. (2019)
GL50803_16343	Median body protein	None	None			X						GFP	Nosala et al. (2019)
GL50803_16424	Mlf1IP domain protein	Mlf1IP	PF10248	X	X	X						GFP	Nosala et al. (2019)
GL50803_13981	Nek kinase GK185	NEK, ankyrin	PF00069, PF12796			X						GFP	Nosala et al. (2019)
GL50803_17231	Nek kinase GK186	NEK, ankyrin	PF00069, PF12796			X						GFP	Nosala et al. (2019)
GL50803_16272	Nek kinase GK187	NEK, ankyrin	PF00069, PF12796			X						GFP	Nosala et al. (2019)
GL50803_10893	Nek kinase GK193	NEK	PF00069		X	X						GFP	Nosala et al. (2019)
GL50803_3957	Nek kinase GK212	NEK, ankyrin	PF00069, PF12796			X						GFP	Nosala et al. (2019)
GL50803_11554	Nek kinase GK249	NEK	PF00069			X						GFP	Nosala et al. (2019)
GL50803_16279	Nek kinase GK256	NEK	PF00069	X	X	X						HOM, EPI	Davids et al. (2011) and Manning et al. (2011)
GL50803_24321	Nek kinase GK261	NEK	PF00069			X						GFP	Nosala et al. (2019)
GL50803_4912	Nek kinase GK265	NEK	PF00069			X						GFP	Nosala et al. (2019)
GL50803_92498	Nek kinase GK270	NEK	PF00069		X	X						EPI	Davids et al. (2011) and Manning et al. (2011)

Adv Parasitol. Author manuscript; available in PMC 2021 April 30.

GiardiaDB	Protein name	Protein family	PFAM	BB	AX	DSC	MB	FN	SN	MS	Other localization	Evidence	References
GL50803_5489	Nek kinase GK271	NEK	PF00069			X						GFP	Nosala et al. (2019)
GL50803_4977	Nek kinase GK282	NEK	PF00069			X						GFP	Nosala et al. (2019)
GL50803_11775	Nek kinase GK301	NEK, ankyrin	PF00069, PF12796	X	X	X						GFP	Nosala et al. (2019)
GL50803_7710	Nek kinase GK445	NEK	PF00069			X						GFP	Dawsonlab (GiardiaDB)
GL50803_4410	SALP-1	SF-assemblin	PF06705			X						GFP	Nosala et al. (2019)
GL50803_17090	SAM domain protein	SAM	PF00546			X						GFP	Nosala et al. (2019)
GL50803_5010	Ser/Thr phosphatase PP2A-2 catalytic subunit	Calcineurin-like phosphoesterase	PF00149	X	X	X						IFA	Lauwaet et al. (2007) and Manning et al. (2011)
GL50803_15410	Ser/Thr protein kinase	Ankyrin repeat domain	PF12796			X						GFP	Nosala et al. (2019)
GL50803_103164	SHIPPO-repeat family protein	SHIPPO-repeat	PF07004		X	X						GFP	Nosala et al. (2019)
GL50803_9148	SHIPPO-repeat family protein	SHIPPO-repeat	PF07004		X	X						GFP	Nosala et al. (2019)
GL50803_5374	Tubulin-specific chaperone B	CAP-GLY	PF01302			X						GFP	Nosala et al. (2019)
GL50803_15218	WD-40 repeat protein	WD-40 repeat protein	PF00400	X	X	X	X					IFA, GFP	Nosala et al. (2019)
Median body-associated													
GL50803_14748	Conserved hypothetical protein	None	None				X				Cytoplasm, nuclei	GFP	Dawsonlab (GiardiaDB)
GL50803_92760	Hypothetical protein	None	None				X	X				GFP	Dawsonlab (GiardiaDB)
GL50803_12224	Hypothetical protein	None	None				X					GFP	Dawsonlab (GiardiaDB)
GL50803_35670	Zinc finger domain containing protein	Zinc finger domain protein	PF16543				X				Cytoplasm	GFP	Dawsonlab (GiardiaDB)
Funis-associated													
GL50803_4657	Hypothetical protein	None	None	X	X			X				GFP	Dawsonlab (GiardiaDB)
GL50803_17266	Hypothetical protein	None	None		X		X	X				GFP	Dawsonlab (GiardiaDB)

Disc-associated proteins (DAPs) have been identified by on homology to known cytoskeletal-associated proteins in other organisms (HOM) or by subcellular localization using heterologous antibodies (IFA), epitope-tagging (EPI), or fluorescent tags (GFP, mNG) (Nosala et al., 2018). Over 90 disc-associated or median body-associated proteins have been localized during an ongoing, publicly available, *Giardia* C-terminal GFP-tagging project for EuPATHDB (Harb and Roos, 2015) conducted in our laboratory (GFP) to the basal bodies (BB), axonemes (AX), disc (DSC), median body (MB), funis (FN), supernumerary MTs (SN) or mitotic spindles (MS).

Table 3

Inventory of conserved and novel flagellar assembly and structural.

	GiardiaDB	Protein name	Protein family	PFAM	BB	AX	DSC	MB	FN	SN	MS	Other localization	Evidence	References
Axoneme assembly														
IFT motors	GL50803_93736	cytoDHC-1b	Dynein heavy chain (DHC) family	PF03028								n.d.	HOM	Wickstead and Gull (2007)
	GL50803_17333	GiKIN2a	Kinesin-2	PF00225	X	X							HOM, GFP	McInally et al. (2020)
	GL50803_16456	GiKIN2b	Kinesin-2	PF00225	X	X							HOM, GFP	McInally et al. (2020)
	GL50803_114885	KAP	Non-motor subunit of kinesin-II complex	PF05804								n.d.	HOM	Morrison et al. (2007)
IFT complex A	GL50803_16547	Intraflagellar transport protein IFT122	WD-40 repeat protein	PF00400	X	X							HOM, GFP	McInally et al. (2020)
	GL50803_17251	Intraflagellar transport protein IFT140	WD-40 repeat protein	PF00400	X	X							HOM, GFP	McInally et al. (2020)
	GL50803_87817	Intraflagellar transport protein IFT121	None	None	X	X							HOM, GFP	McInally et al. (2020)
IFT complex B	GL50803_14713	Intraflagellar transport protein IFT57	IFT57	PF10498	X	X							HOM, GFP	McInally et al. (2020)
	GL50803_9750	Intraflagellar transport protein IFT74/72	None	None	X	X							HOM, GFP	McInally et al. (2020)
	GL50803_15428	Intraflagellar transport protein IFT81	None	None	X	X							HOM, GFP	McInally et al. (2020)
	GL50803_16660	Intraflagellar transport protein IFT88	None	None	X	X							HOM, GFP	McInally et al. (2020)
	GL50803_17105	Intraflagellar transport protein IFT172	None	None	X	X							HOM, GFP	McInally et al. (2020)
	GL50803_17223	Intraflagellar transport protein IFT180	WD-40 repeat protein	PF00400	X	X							HOM, GFP	McInally et al. (2020)

	GiardiaDB	Protein name	Protein family	PFAM	BB	AX	DSC	MB	FN	SN	MS	Other localization	Evidence	References
	GL50803_7664	Intraflagellar transport protein IFT46	IFT46	PF12317								n.d.	HOM	Morrison et al. (2007)
	GL50803_40995	Intraflagellar transport protein IFT52	Intraflagellar transport protein IFT52	None								n.d.	HOM	Morrison et al. (2007)
	GL50803_16707	Intraflagellar transport protein IFT38	Cluap1 family protein	PF10234	X	X							HOM, GFP	McInally et al. (2020)
	GL50803_9098	Intraflagellar transport protein IFT54	None	None	X	X							HOM, GFP	McInally et al. (2020)
	GL50803_16375	Intraflagellar transport protein IFT56	TPR_1 tetratricopeptide repeat	PF13432	X	X							HOM, GFP	McInally et al. (2020)
Axoneme-associated														
Central pair Radial spokes	GL50803_16202	Axoneme central apparatus protein PF16/SPAG6	Central pair associated protein	PF00514	X	X							HOM, IFA, EPI	House et al. (2011) and Lauwaet et al. (2011)
	GL50803_137712	HY3 (FAP74)	HYD3	SSF52540								n.d.	HOM	Morrison et al. (2007)
	GL50803_16500	PF20	Central pair WD-repeat protein	PF00400								n.d.	HOM	Morrison et al. (2007)
	GL50803_14568	PP1	Ser/Thr protein phosphatase PP1-alpha 2 catalytic subunit	SSF56300								n.d.	HOM	Morrison et al. (2007)
	GL50803_114462	Axonemal p66 (RSP6)	Outer dynein arm-docking complex subunit 2 (ODA-DC 2)	None		X							HOM, GFP	Dawsonlab (GiardiaDB)
	GL50803_16450	rsp3	Radial spoke protein 3	PF06098								n.d.	HOM	Morrison et al. (2007)
	GL50803_17278	rsp9	Radial spoke protein 9; (pf17)	None								n.d.	HOM	Morrison et al. (2007)
	GL50803_16720	Radial spokehead family protein	Radial spokehead family protein	PF04712		X							GFP	Dawsonlab (GiardiaDB)
Other axoneme-associated	GL50803_7009	Adenylate kinase family protein	AAA domain	PF13238		X							GFP	Dawsonlab (GiardiaDB)

Adv Parasitol. Author manuscript; available in PMC 2021 April 30.

GiardiaDB	Protein name	Protein family	PFAM	BB	AX	DSC	MB	FN	SN	MS	Other localization	Evidence	References
GL50803_86444	AGC family kinase	AGC kinase	PF00069	X	X							EPI	Morrison et al. (2007) and Manning et al. (2011)
GL50803_5649	Alpha10-giardin	Annexin	PF00191		X							HOM, EPI, IFA	Weiland et al. (2005)
GL50803_10073	Alpha12-giardin	Annexin	PF00191		X							HOM, IFA	Wu et al. (2016)
GL50803_15097	Alpha14-giardin	Annexin	PF00191		X							HOM, EPI	Weiland et al. (2005)
GL50803_10038	Alpha18-giardin	Annexin	PF00191		X							HOM, EPI	Weiland et al. (2005) and Wu et al. (2016)
GL50803_103437	Alpha9-giardin	Annexin	PF00191		X							HOM, EPI	Weiland et al. (2005)
GL50803_14741	Ankyrin repeat protein	Ankyrin repeat domain	PF12796	X	X							GFP	Dawsonlab (GiardiaDB)
GL50803_17586	Ankyrin repeat protein	Ankyrin repeat domain	PF12796	X	X							GFP	Dawsonlab (GiardiaDB)
GL50803_24412	Ankyrin repeat protein	Ankyrin repeat domain	PF12796	X	X							GFP	Dawsonlab (GiardiaDB)
GL50803_102023	Ankyrin repeat protein	Ankyrin repeat domain	PF12796		X						Marginal plate	GFP	Dawsonlab (GiardiaDB)
GL50803_9722	Ankyrin repeat protein	Ankyrin repeat domain	PF12796		X						Marginal plate	GFP	Dawsonlab (GiardiaDB)
GL50803_14133	Ankyrin repeat protein	Ankyrin repeat domain	PF12796		X							GFP	Dawsonlab (GiardiaDB)
GL50803_15456	Ankyrin repeat protein	Ankyrin repeat domain	PF12796		X							GFP	Dawsonlab (GiardiaDB)
GL50803_7021	Ankyrin repeat protein	Ankyrin repeat domain	PF12796		X							GFP	Dawsonlab (GiardiaDB)
GL50803_101168	Ankyrin repeat protein	Ankyrin repeat domain	PF12796		X							GFP	Dawsonlab (GiardiaDB)
GL50803_17402	Ankyrin repeat protein	Ankyrin repeat domain	PF12796		X							GFP	Dawsonlab (GiardiaDB)
GL50803_27836	Ankyrin repeat protein	Ankyrin repeat domain	PF12796		X							GFP	Dawsonlab (GiardiaDB)
GL50803_9117	CAMP-dependent protein kinase regulatory chain	Cyclic nucleotide binding domain	PF00027	X	X							EPI	Morrison et al. (2007) and

GiardiaDB	Protein name	Protein family	PFAM	BB	AX	DSC	MB	FN	SN	MS	Other localization	Evidence	References
													Manning et al. (2011)
GL50803_16802	CDK kinase (CMGC family)	CDK (CMGC family)	PF00069	X	X						Plasma membrane	GFP	Dawsonlab (GiardiaDB)
GL50803_13262	CLAMP superfamily protein	CLAMP superfamily protein	PF14769		X						Plasma membrane	GFP	Dawsonlab (GiardiaDB)
GL50803_16707	Cluap1 family protein	Cluap1 family protein	PF10234		X							GFP	Dawsonlab (GiardiaDB)
GL50803_16013	Conserved hypothetical protein	None	None		X	X	X				Nuclei	GFP	Dawsonlab (GiardiaDB)
GL50803_6377	Conserved hypothetical protein	None	None		X						Cytoplasm	GFP	Dawsonlab (GiardiaDB)
GL50803_8626	Conserved hypothetical protein	None	None		X						Cytoplasm	GFP	Dawsonlab (GiardiaDB)
GL50803_13288	Conserved hypothetical protein	None	None		X							GFP	Dawsonlab (GiardiaDB)
GL50803_15995	Conserved hypothetical protein	None	None		X							GFP	Dawsonlab (GiardiaDB)
GL50803_16998	Conserved hypothetical protein	None	None		X							GFP	Dawsonlab (GiardiaDB)
GL50803_9098	Conserved hypothetical protein	None	None		X							GFP	Dawsonlab (GiardiaDB)
GL50803_9427	Conserved hypothetical protein	None	None		X							GFP	Dawsonlab (GiardiaDB)
GL50803_21110	dpy-30 domain protein	dpy-30 domain protein	PF05186		X		X		X			GFP	Dawsonlab (GiardiaDB)
GL50803_4538	dpy-30 domain protein	dpy-30 domain protein	PF05186		X						Plasma membrane	GFP	Dawsonlab (GiardiaDB)
GL50803_3582	DUF390 domain containing protein	DUF390	PF04094	X	X							GFP	Dawsonlab (GiardiaDB)
GL50803_4624	DUF4490 domain containing protein	DUF4490	PF14892	X	X		X					GFP	Dawsonlab (GiardiaDB)

GiardiaDB	Protein name	Protein family	PFAM	BB	AX	DSC	MB	FN	SN	MS	Other localization	Evidence	References
GL50803_8423	Enkurin superfamily protein	Enkurin superfamily protein	PF13864		X	X					Nuclear membrane	GFP	Dawsonlab (GiardiaDB)
GL50803_16996	Enkurin superfamily protein	Enkurin superfamily protein	PF13864		X		X					GFP	Dawsonlab (GiardiaDB)
GL50803_6897	ERC protein 2 family protein	ERC protein 2 family protein	None		X							GFP	Dawsonlab (GiardiaDB)
GL50803_13372	FAP45	TPH domain	PF13868								n.d.	HOM	Keller et al. (2005)
GL50803_15956	FAP52	WD-40 repeat protein	PF00400		X						Plasma membrane	HOM, GFP	Dawsonlab (GiardiaDB)
GL50803_7192	FWWh domain containing protein	FWWh domain of unknown function	PF14922	X	X							GFP	Dawsonlab (GiardiaDB)
GL50803_137716	GASP-180	Ankyrin repeat domain	PF00023		X						Cytoplasm	IFA, GFP	Elmendorf et al. (2005)
GL50803_17109	Hypothetical protein	None	None	X	X	X					Cytoplasm	GFP	Dawsonlab (GiardiaDB)
GL50803_10460	Hypothetical protein	None	None	X	X		X					GFP	Dawsonlab (GiardiaDB)
GL50803_15446	Hypothetical protein	None	None	X	X		X					GFP	Dawsonlab (GiardiaDB)
GL50803_17154	Hypothetical protein	None	None	X	X		X					GFP	Dawsonlab (GiardiaDB)
GL50803_29796	Hypothetical protein	None	None	X	X		X					GFP	Dawsonlab (GiardiaDB)
GL50803_8974	Hypothetical protein	None	None	X	X		X					GFP	Dawsonlab (GiardiaDB)
GL50803_31185	Hypothetical protein	None	None	X	X		X					GFP	Dawsonlab (GiardiaDB)
GL50803_16973	Hypothetical protein	None	None	X	X		X					IFA	Lauwaet et al. (2011)
GL50803_16811	Hypothetical protein	None	None	X	X						Lateral shield	GFP	Dawsonlab (GiardiaDB)
GL50803_114546	Hypothetical protein	None	None	X	X							GFP	Dawsonlab (GiardiaDB)
GL50803_6254	Hypothetical protein	None	None	X	X							GFP	Dawsonlab (GiardiaDB)

GiardiaDB	Protein name	Protein family	PFAM	BB	AX	DSC	MB	FN	SN	MS	Other localization	Evidence	References
GL50803_7351	Hypothetical protein	None	None	X	X							GFP	Dawsonlab (GiardiaDB)
GL50803_8557	Hypothetical protein	None	None	X	X							GFP	Dawsonlab (GiardiaDB)
GL50803_13809	Hypothetical protein	None	None	X	X							GFP	Dawsonlab (GiardiaDB)
GL50803_29252	Hypothetical protein	None	None	X	X							GFP	Dawsonlab (GiardiaDB)
GL50803_15139	Hypothetical protein	None	None		X	X					Cytoplasm	GFP	Dawsonlab (GiardiaDB)
GL50803_3158	Hypothetical protein	None	None		X		X				Plasma membrane	GFP	Dawsonlab (GiardiaDB)
GL50803_14967	Hypothetical protein	None	None		X		X					GFP	Dawsonlab (GiardiaDB)
GL50803_16236	Hypothetical protein	None	None		X		X					GFP	Dawsonlab (GiardiaDB)
GL50803_20168	Hypothetical protein	None	None		X		X					GFP	Dawsonlab (GiardiaDB)
GL50803_7825	Hypothetical protein	None	None		X		X					GFP	Dawsonlab (GiardiaDB)
GL50803_87577	Hypothetical protein	None	None		X		X					GFP	Dawsonlab (GiardiaDB)
GL50803_14895	Hypothetical protein	None	None		X						Cytoplasm	GFP	Dawsonlab (GiardiaDB)
GL50803_8854	Hypothetical protein	None	None		X						Marginal plate	GFP	Dawsonlab (GiardiaDB)
GL50803_15367	Hypothetical protein	None	None		X						Nuclei	GFP	Dawsonlab (GiardiaDB)
GL50803_28526	Hypothetical protein	None	None		X						Nuclei	GFP	Dawsonlab (GiardiaDB)
GL50803_15847	Hypothetical protein	None	None		X						Plasma membrane	GFP	Dawsonlab (GiardiaDB)
GL50803_10697	Hypothetical protein	None	None		X							GFP	Dawsonlab (GiardiaDB)
GL50803_10850	Hypothetical protein	None	None		X							GFP	Dawsonlab (GiardiaDB)
GL50803_11327	Hypothetical protein	None	None		X							GFP	Dawsonlab (GiardiaDB)

GiardiaDB	Protein name	Protein family	PFAM	BB	AX	DSC	MB	FN	SN	MS	Other localization	Evidence	References
GL50803_13210	Hypothetical protein	None	None		X							GFP	Dawsonlab (GiardiaDB)
GL50803_13584	Hypothetical protein	None	None		X							GFP	Dawsonlab (GiardiaDB)
GL50803_14045	Hypothetical protein	None	None		X							GFP	Dawsonlab (GiardiaDB)
GL50803_14481	Hypothetical protein	None	None		X							GFP	Dawsonlab (GiardiaDB)
GL50803_14947	Hypothetical protein	None	None		X							GFP	Dawsonlab (GiardiaDB)
GL50803_14963	Hypothetical protein	None	None		X							GFP	Dawsonlab (GiardiaDB)
GL50803_14971	Hypothetical protein	None	None		X							GFP	Dawsonlab (GiardiaDB)
GL50803_17058	Hypothetical protein	None	None		X							GFP	Dawsonlab (GiardiaDB)
GL50803_17531	Hypothetical protein	None	None		X							GFP	Dawsonlab (GiardiaDB)
GL50803_17571	Hypothetical protein	None	None		X							GFP	Dawsonlab (GiardiaDB)
GL50803_20603	Hypothetical protein	None	None		X							GFP	Dawsonlab (GiardiaDB)
GL50803_27887	Hypothetical protein	None	None		X							GFP	Dawsonlab (GiardiaDB)
GL50803_3896	Hypothetical protein	None	None		X							GFP	Dawsonlab (GiardiaDB)
GL50803_4590	Hypothetical protein	None	None		X							GFP	Dawsonlab (GiardiaDB)
GL50803_7696	Hypothetical protein	None	None		X							GFP	Dawsonlab (GiardiaDB)
GL50803_7876	Hypothetical protein	None	None		X							GFP	Dawsonlab (GiardiaDB)
GL50803_8135	Hypothetical protein	None	None		X							GFP	Dawsonlab (GiardiaDB)
GL50803_8358	Hypothetical protein	None	None		X							GFP	Dawsonlab (GiardiaDB)
GL50803_86855	Hypothetical protein	None	None		X							GFP	Dawsonlab (GiardiaDB)

GiardiaDB	Protein name	Protein family	PFAM	BB	AX	DSC	MB	FN	SN	MS	Other localization	Evidence	References
GL50803_8725	Hypothetical protein	None	None		X							GFP	Dawsonlab (GiardiaDB)
GL50803_8821	Hypothetical protein	None	None		X							GFP	Dawsonlab (GiardiaDB)
GL50803_13133	Hypothetical protein	None	None		X		X					GFP	Dawsonlab (GiardiaDB)
GL50803_17249	Hypothetical protein	None	None		X							GFP	Dawsonlab (GiardiaDB)
GL50803_17536	Hypothetical protein	None	None		X							GFP	Dawsonlab (GiardiaDB)
GL50803_93278	Importin beta domain protein	Importin beta domain protein	PF01749		X						Nuclear membrane	GFP	Dawsonlab (GiardiaDB)
GL50803_14004	Long-flagella protein LF4	MAP kinase	PF00069								n.d.	HOM	Morrison et al. (2007)
GL50803_137749	LRR domain protein	LRR domain protein	PF00560		X							GFP	Dawsonlab (GiardiaDB)
GL50803_15219	Macoilin domain containing protein	Macoilin	PF09726	X	X							GFP	Dawsonlab (GiardiaDB)
GL50803_102248	MBO2	MBO2 domain	PD936484	X							n.d.	HOM	Morrison et al. (2007)
GL50803_5375	Nek kinase GK170	NEK	PF00069		X							GFP	Dawsonlab (GiardiaDB)
GL50803_5643	Nek kinase GK181	NEK	PF00069		X						Plasma membrane	GFP	Dawsonlab (GiardiaDB)
GL50803_4897	Nek kinase GK184	NEK	PF00069	X	X							GFP	Dawsonlab (GiardiaDB)
GL50803_2082	Nek kinase GK199	NEK	PF00069		X						Marginal plate	GFP	Dawsonlab (GiardiaDB)
GL50803_114192	Nek kinase GK400	NEK	PF00069		X							GFP	Dawsonlab (GiardiaDB)
GL50803_11311	Nek kinase GL169	NEK-GL2	PF00069		X							GFP	Dawsonlab (GiardiaDB)
GL50803_14135	Nucleoside diphosphate kinase	Nucleoside diphosphate kinase	PF00334		X							GFP	Dawsonlab (GiardiaDB)
GL50803_16237	NYD-SP28 domain protein	NYD-SP28 domain protein	PF14772		X							GFP	Dawsonlab (GiardiaDB)

	GiardiaDB	Protein name	Protein family	PFAM	BB	AX	DSC	MB	FN	SN	MS	Other localization	Evidence	References
	GL50803_15455	PACRG1	Parkin coregulated protein	PF10274								Cytoplasm, nuclei	HOM, GFP	Dawsonlab (GiardiaDB)
	GL50803_33762	POC1	WD-40 repeat protein	PF00400								n.d.	HOM	Keller et al. (2005)
	GL50803_32375	POC18	None	None		X	n.d.						HOM	Keller et al. (2005)
	GL50803_7439	PP2A	Ser/Thr phosphatase 2A	SSF48371								n.d.	HOM	Morrison et al. (2007)
	GL50803_11867	RIB43A	RIB43A	PF05914	X	X		X					EPI, GFP	Lauwaet et al. (2011), Dawsonlab (GiardiaDB)
	GL50803_31671	RPB7 SHS2 domain containing protein	RPB7 SHS2 domain	PF03876	X	X							GFP	Dawsonlab (GiardiaDB)
	GL50803_2833	spc25	Spindle-associated spc25	PF08234		X							GFP	Dawsonlab (GiardiaDB)
	GL50803_13352	TPR domain containing protein	TPR domain	PF07202	X	X							IFA, GFP	Lauwaet et al. (2011)
	GL50803_5167	VFL3	None	None		X						n.d.	HOM	Merchant et al. (2007)
	GL50803_7807	WD-40 repeat protein	WD-40 repeat protein	PF00400		X						Cytoplasm	GFP	Dawsonlab (GiardiaDB)
	GL50803_15956	WD-40 repeat protein	WD-40 repeat protein	PF00400		X						Plasma membrane	GFP	Dawsonlab (GiardiaDB)
	GL50803_17068	WD-40 repeat protein	WD-40 repeat protein	PF00400		X							GFP	Dawsonlab (GiardiaDB)

More than 150 flagellar proteins are identifiable in the *Giardia lamblia* (ATCC 50803) genome (Morrison et al., 2007), including IFT complex A and B, microtubule and dynein motors, and structural components of the axonemes, central pair MTs, and radial spokes. Flagellar proteins have been identified and verified from homology to homologues in other organisms (HOM) or by subcellular localization using heterologous antibodies (IFA), epitope-tagging (EPI), or fluorescent tags (GFP, mNG). Many Giardia-specific axoneme-associated proteins have been localized during an ongoing, publicly available, *Giardia* C-terminal GFP-tagging project for EuPATHDB (Harb and Roos, 2015) conducted in our laboratory (GFP) to the basal bodies (BB), axonemes (AX), disc (DSC), median body (MB), funis (FN), supernumerary MTs (SN) or mitotic spindles (MS).